Article

Neutralizing antibody vaccine for pandemic and pre-emergent coronaviruses

https://doi.org/10.1038/s41586-021-03594-0

Received: 7 February 2021

Accepted: 29 April 2021

Published online: 10 May 2021

Check for updates

Kevin O. Saunders[1,2,3,4]✉, Esther Lee[1,5], Robert Parks[1,5], David R. Martinez[6], Dapeng Li[1,5], Haiyan Chen[1,5], Robert J. Edwards[1,5], Sophie Gobeil[1,5], Maggie Barr[1,5], Katayoun Mansouri[1,5], S. Munir Alam[1,5], Laura L. Sutherland[1,5], Fangping Cai[1,5], Aja M. Sanzone[1,5], Madison Berry[1,5], Kartik Manne[1,5], Kevin W. Bock[7], Mahnaz Minai[7], Bianca M. Nagata[7], Anyway B. Kapingidza[1,5], Mihai Azoitei[1,5], Longping V. Tse[6], Trevor D. Scobey[6], Rachel L. Spreng[1,5], R. Wes Rountree[1,5], C. Todd DeMarco[1,5], Thomas N. Denny[1,5], Christopher W. Woods[1,5,8], Elizabeth W. Petzold[8], Juanjie Tang[9], Thomas H. Oguin III[1,5], Gregory D. Sempowski[1,5], Matthew Gagne[10], Daniel C. Douek[10], Mark A. Tomai[11], Christopher B. Fox[12], Robert Seder[10], Kevin Wiehe[1,5], Drew Weissman[13], Norbert Pardi[13], Hana Golding[9], Surender Khurana[9], Priyamvada Acharya[1,2], Hanne Andersen[14], Mark G. Lewis[14], Ian N. Moore[7], David C. Montefiori[1,2], Ralph S. Baric[6] & Barton F. Haynes[1,3,5]✉

Betacoronaviruses caused the outbreaks of severe acute respiratory syndrome (SARS) and Middle East respiratory syndrome, as well as the current pandemic of SARS coronavirus 2 (SARS-CoV-2)[1–4]. Vaccines that elicit protective immunity against SARS-CoV-2 and betacoronaviruses that circulate in animals have the potential to prevent future pandemics. Here we show that the immunization of macaques with nanoparticles conjugated with the receptor-binding domain of SARS-CoV-2, and adjuvanted with 3M-052 and alum, elicits cross-neutralizing antibody responses against bat coronaviruses, SARS-CoV and SARS-CoV-2 (including the B.1.1.7, P.1 and B.1.351 variants). Vaccination of macaques with these nanoparticles resulted in a 50% inhibitory reciprocal serum dilution (ID_{50}) neutralization titre of 47,216 (geometric mean) for SARS-CoV-2, as well as in protection against SARS-CoV-2 in the upper and lower respiratory tracts. Nucleoside-modified mRNAs that encode a stabilized transmembrane spike or monomeric receptor-binding domain also induced cross-neutralizing antibody responses against SARS-CoV and bat coronaviruses, albeit at lower titres than achieved with the nanoparticles. These results demonstrate that current mRNA-based vaccines may provide some protection from future outbreaks of zoonotic betacoronaviruses, and provide a multimeric protein platform for the further development of vaccines against multiple (or all) betacoronaviruses.

SARS-CoV, SARS-CoV-2 and Middle East respiratory syndrome coronavirus (MERS-CoV) emerged from transmission events in which humans were infected with bat or camel coronaviruses[5–8]. Betacoronaviruses that circulate in civets, bats and Malayan pangolins are genetically similar to SARS-CoV and SARS-CoV-2, and use human ACE2 as a receptor[5,6,9–11]; these SARS-related coronaviruses have the potential to be transmitted to humans[12]. Cross-neutralizing antibodies (cross-nAbs) that are capable of neutralizing multiple betacoronaviruses, and of preventing or treating betacoronavirus infection, have been isolated from humans infected with SARS-CoV[13–24], which provides proof-of-concept for the development of vaccines against members of the *Sarbecovirus* subgenus[25].

In mice, the induction of cross-nAbs though vaccination has previously been reported for coronavirus pseudoviruses[26,27]. However, it is unknown whether the vaccination of primates with spike protein can elicit cross-nAbs against SARS-CoV, bat betacoronaviruses or SARS-CoV-2 escape viruses. One target of cross-nAbs is the receptor-binding domain (RBD) of the spike protein[14,24,25]: for example, the antibody DH1047 is a cross-nAb that targets the RBD and cross-neutralizes SARS-CoV, SARS-CoV-2 and bat coronaviruses[15]. RBD immunogenicity can be augmented by arraying multiple copies of the domain on nanoparticles, which mimics virus-like particles[26–29]. We therefore designed a vaccine that comprised a 24-mer SARS-CoV-2 RBD nanoparticle conjugated to a ferritin scaffold. We constructed the

[1]Duke Human Vaccine Institute, Duke University School of Medicine, Durham, NC, USA. [2]Department of Surgery, Duke University, Durham, NC, USA. [3]Department of Immunology, Duke University School of Medicine, Durham, NC, USA. [4]Department of Molecular Genetics and Microbiology, Duke University School of Medicine, Durham, NC, USA. [5]Department of Medicine, Duke University School of Medicine, Durham, NC, USA. [6]Department of Epidemiology, University of North Carolina at Chapel Hill, Chapel Hill, NC, USA. [7]Infectious Disease Pathogenesis Section, Comparative Medicine Branch, National Institute of Allergy and Infectious Diseases (NIAID), National Institutes of Health (NIH), Bethesda, MD, USA. [8]Center for Applied Genomics and Precision Medicine, Duke University Medical Center, Durham, NC, USA. [9]Division of Viral Products, Center for Biologics Evaluation and Research (CBER), Food and Drug Administration, Silver Spring, MD, USA. [10]Vaccine Research Center, NIAID, NIH, Bethesda, MD, USA. [11]Corporate Research Materials Lab, 3M Company, St Paul, MN, USA. [12]Infectious Disease Research Institute, Seattle, WA, USA. [13]Department of Medicine, University of Pennsylvania, Philadelphia, PA, USA. [14]BIOQUAL, Rockville, MD, USA. ✉e-mail: kevin.saunders@duke.edu; barton.haynes@duke.edu

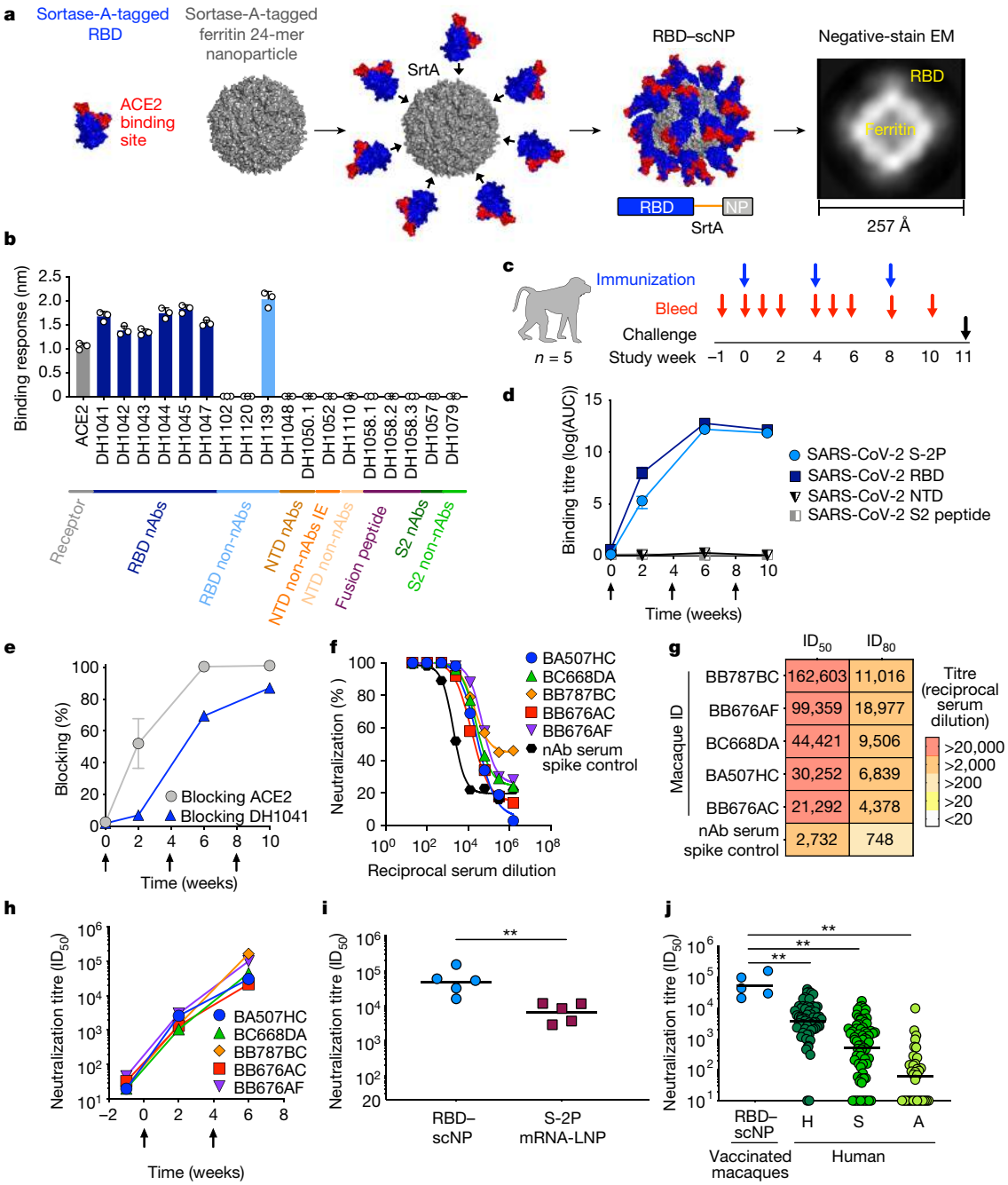

Fig. 1 | RBD–scNP elicits extremely high titres of SARS-CoV-2-pseudovirus neutralizing antibodies. a, SARS-CoV-2 RBD (blue and red)–*H. pylori* ferritin (grey) nanoparticle sortase (SrtA) conjugation. Model and two-dimensional class average of negative-stain electron microscopy (EM) of the resultant RBD–scNP are shown. **b**, Biolayer interferometry SARS-CoV-2 antibody and ACE2-receptor binding to RBD nanoparticles. nAbs, neutralizing antibodies; non-nAbs, non-neutralizing antibodies; non-nAbs IE, infection-enhancing non-neutralizing antibody; NTD, N-terminal domain. Symbols represent values from three independent experiments; data are mean + s.e.m. **c**, Design of the cynomolgus macaque immunogenicity and challenge study. **d**, Macaque serum IgG binding titre as area-under-the-curve (AUC) of the $\log_{10}$-transformed curve (log(AUC)) to recombinant SARS-CoV-2 S-2P, RBD, NTD and fusion peptide. Group mean ± s.e.m. are shown in **d**, **e** ($n = 5$ macaques). **e**, Plasma antibody blocking of SARS-CoV-2 S-2P binding to ACE2 and RBD neutralizing antibody DH1041. **f**, **g**, Dose-dependent serum neutralization of SARS-CoV-2 D614G pseudovirus infection of ACE2-expressing 293T cells (**f**) and neutralization ID_{50} and ID_{80} titres (**g**). Serum was examined after two immunizations. The mean value of duplicates is shown in **f**. **h**, SARS-CoV-2 D614G pseudovirus serum neutralization titre over time for individual macaques. **i**, Serum neutralization ID_{50} titres from macaques immunized twice with RBD–scNP (blue) or S-2P mRNA-LNP (burgundy). $^{**}P = 0.0079$, two-tailed exact Wilcoxon test. $n = 5$ macaques. **j**, Serum neutralization titres for macaques immunized twice with RBD–scNP (blue) ($n = 5$ macaques) or humans with asymptomatic infection ($n = 34$ individuals) (A), symptomatic infection ($n = 71$ individuals) (S) or who were hospitalized ($n = 60$ individuals) (H). $^{**}P < 0.01$, two-tailed Wilcoxon test. Horizontal bars are the group geometric mean in **i**, **j**. Pre-vaccination serum or neutralizing antibody spiked serum were used as controls in **f**–**h**. **d**, **e**, **h**, Arrows, time of immunization.

RBD nanoparticle by expressing recombinant SARS-CoV-2 RBD with a C-terminal sortase A donor sequence, and by expressing a 24-subunit, self-assembling *Helicobacter pylori* ferritin with an N-terminal sortase A acceptor sequence[30]. We then conjugated the RBD to ferritin nanoparticles using a sortase A reaction[30] (Fig. 1a, Extended Data Fig. 1). We used analytical size-exclusion chromatography and negative-stain

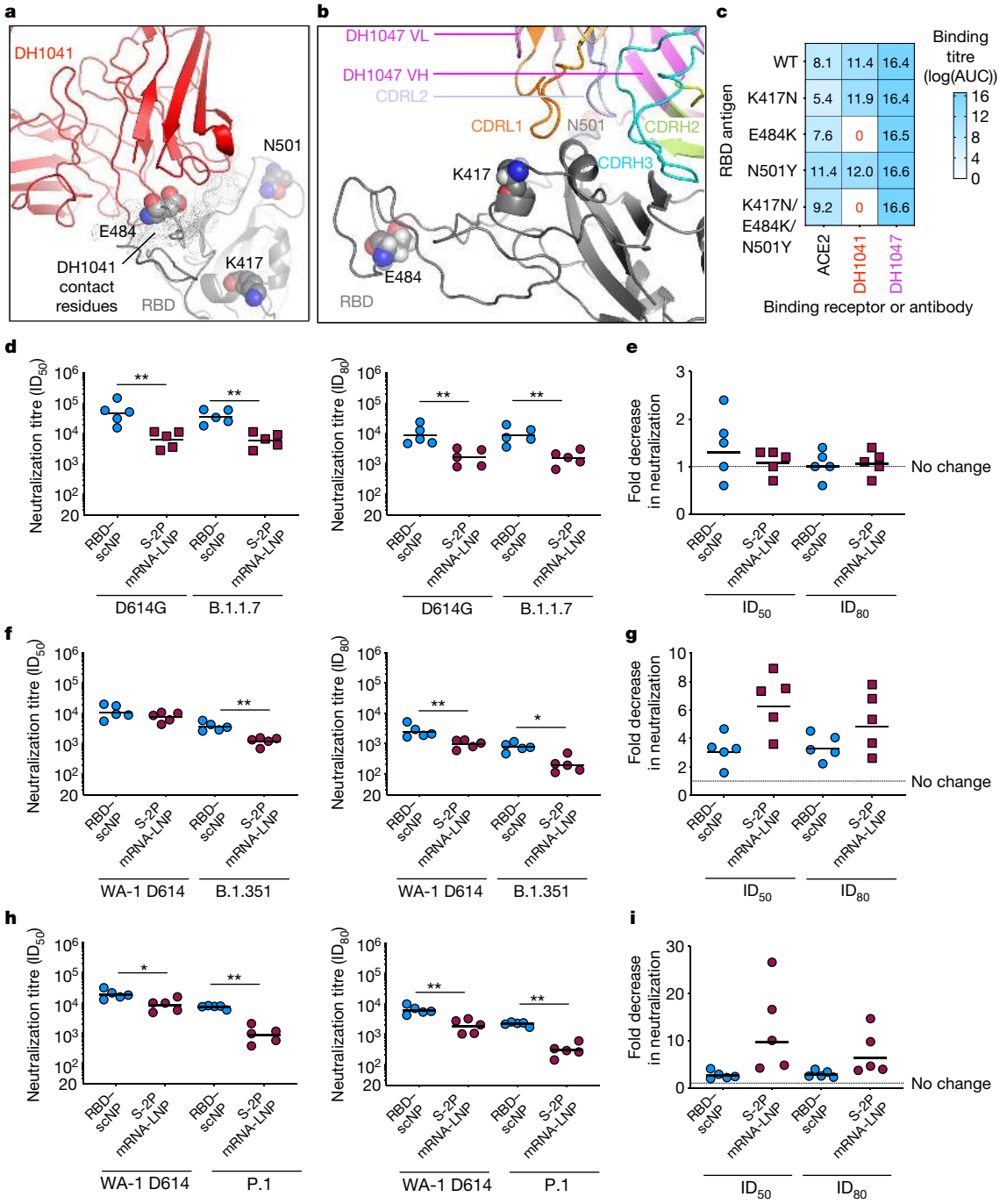

Fig. 2 | RBD–scNP elicits a higher titre of neutralizing antibodies against more transmissible or neutralization-resistant SARS-CoV-2 variants than does S-2P mRNA-LNP. a, **b**, The location of K417, E484 and N501 (spheres), which are mutated in the B.1.351 variant, are shown in the cryo-electron microscopy structures of the RBD neutralizing antibodies DH1041 (red) (**a**) and DH1047 (magenta) (**b**) bound to the RBD (grey) of spike trimers (Protein Data Bank codes (PDB) 7LAA and 7LD1)[15]. **c**, ACE2 receptor, DH1041 and DH1047 enzyme-linked immunosorbent assay (ELISA) binding titre as log(AUC), for wild-type (WT) and mutant SARS-CoV-2 spike RBD monomers. **d**, Serum neutralization ID_{50} (left) and ID_{80} (right) titres for SARS-CoV-2 D614G and SARS-CoV-2 B.1.1.7 pseudoviruses from immunized macaques, in ACE2-expressing 293 cells. Symbols represent individual macaques; horizontal bars are group means. $^{**}P = 0.0079$, two-tailed exact Wilcoxon test. $n = 5$ macaques. **e**, Fold decrease in neutralization potency in neutralization of SARS-CoV-2 B.1.1.7 pseudovirus relative to SARS-CoV-2 D614G pseudovirus. Fold change is shown for RBD–scNP-immunized and S-2P mRNA-LNP-immunized macaques on the basis of the ID_{50} and ID_{80} titres. Horizontal bars are the group mean. **f**, Vaccinated macaque serum neutralization ID_{50} (left) and ID_{80} titres (right) against SARS-CoV-2 WA-1 and B.1.351 pseudoviruses, in ACE2-expressing 293 cells. Symbols and horizontal bars are shown the same as in **d**. $^{*}P = 0.0159$; $^{**}P = 0.0079$, two-tailed exact Wilcoxon test. $n = 5$ macaques. **g**, Fold decrease in neutralization potency in neutralization of SARS-CoV-2 B.1.351 pseudovirus relative to SARS-CoV-2 WA-1 pseudovirus. Fold change is shown as in **e**. **h**, Vaccine-induced ID_{50} (left) and ID_{80} (right) neutralization titres of infection of ACE2- and TMPRSS2-expressing 293 cells by SARS-CoV-2 WA-1 or P.1 pseudovirus. Symbols and horizontal bars are as in **d**. $^{*}P = 0.0159$; $^{**}P = 0.0079$, two-tailed exact Wilcoxon test. $n = 5$ macaques. **i**, Fold decrease in neutralization potency (as shown in **e**) for SARS-CoV-2 P.1 pseudovirus relative to SARS-CoV-2 WA-1 pseudovirus.

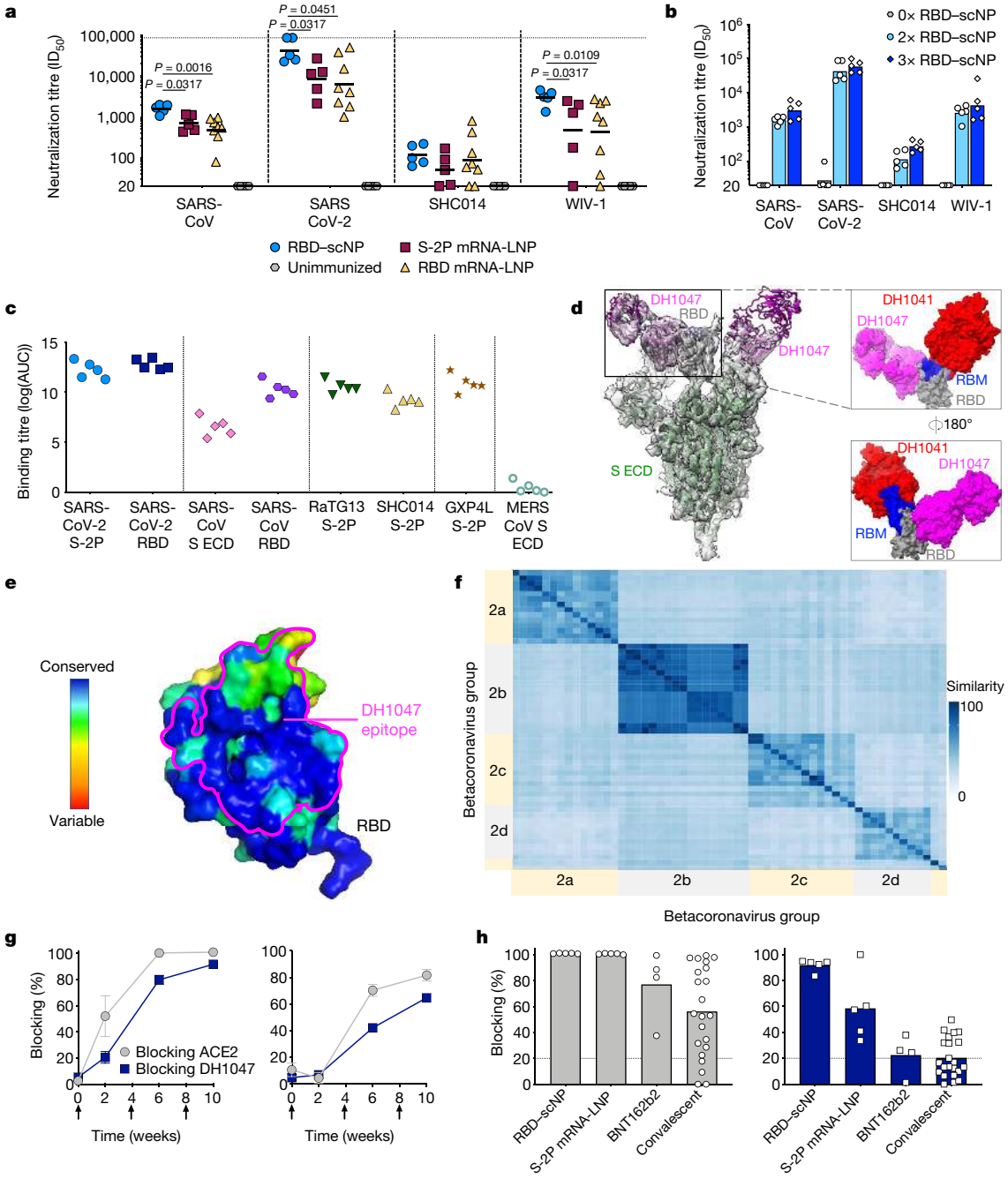

Fig. 3 | Serum cross-neutralization of infections with SARS-related betacoronaviruses induced by RBD–scNP. a, Serum neutralization ID_{50} titres from macaques immunized twice with RBD–scNP, S-2P mRNA-LNP or RBD mRNA-LNP for SARS-CoV, SARS-CoV-2 and SARS-related bat coronaviruses (WIV-1 and SHC014) infections. Symbols indicate individual macaques; black bars show the group geometric mean. Two-tailed exact Wilcoxon test, $n = 5$ or 8 macaques. **b**, Serum cross-neutralization ID_{50} titres before (grey), or after two (light blue) or three (blue), RBD–scNP immunizations. Bars represent the group geometric mean. **c**, Binding titre (log(AUC)), based on ELISA for the spike protein of human, bat (RaTG13 and SHC014) and pangolin (GXP4L) SARS-related betacoronaviruses, for plasma IgG from macaques immunized twice with RBD–scNP. ECD, ectodomain; S, spike. **d**, Structural comparison of the epitopes of SARS-CoV-2-specific neutralizing RBD antibody (DH1041) (red) (PDB 7LAA) and cross-neutralizing RBD antibody (DH1047) (magenta) (PDB 7LD1). Left, cartoon view of spike (green), RBD (grey) and receptor binding motif (RBM) (blue). Right, overlay of the RBDs of the two complexes from their respective cryo-electron microscopy structures. **e**, RBD coloured by conservation within group-2b betacoronaviruses. DH1047 epitope is shown in magenta outline. **f**, RBD sequence conservation. Heat map displaying pairwise amino acid sequence similarity for 57 representative betacoronaviruses. **g**, **h**, Plasma or serum antibody blocking of S-2P binding to ACE2 (grey) and DH1047 (navy blue). **g**, Plasma antibody inhibition of spike binding. SARS-CoV-2 S-2P (left) or SHC014 S-2P (right) blocking kinetics by serum from macaques immunized twice with RBD–scNP. Group mean ± s.e.m. is shown. $n = 5$ macaques. Arrows, time of immunization. **h**, Blocking of SARS-CoV-2 S-2P binding to ACE2 (left) or DH1047 (right). Blocking activity by serum from macaques immunized twice with RBD–scNP or S-2P mRNA-LNP, and humans immunized twice with Pfizer BNT162b2 (BNT162b) or naturally infected with SARS-CoV-2 (convalescent). Each symbol represents an individual and filled bars indicate the group mean in **h**. Positivity threshold (dashed line) is greater than 20% in **h**.

electron microscopy to confirm that the RBD was conjugated to the surface of the ferritin nanoparticle (Fig. 1a, Extended Data Fig. 1b, c). The RBD sortase-A-conjugated nanoparticle (hereafter, RBD–scNP) bound to human ACE2 (the receptor for SARS-CoV-2) and to potent neutralizing SARS-CoV-2-specific RBD antibodies DH1041, DH1042, DH1043, DH1044 and DH1045[15] (Fig. 1b). The cross-nAb DH1047 also bound to the RBD–scNP (Fig. 1b). The RBD–scNP lacked binding to SARS-CoV-2 spike antibodies that bound outside of the RBD (Fig. 1b).

We immunized five cynomolgus macaques three times intramuscularly, four weeks apart, with 100 μg of RBD–scNP adjuvanted with 5 μg of the TLR7 and TLR8 agonist 3M-052 absorbed to 500 μg of alum[31] (Fig. 1c, Extended Data Fig. 1d, e). Immunizations were well-tolerated in macaques (Extended Data Fig. 2). Immunization with RBD–scNP adjuvanted with 3M-052 and alum elicited binding IgG against both the SARS-CoV-2 RBD and the spike ectodomain stabilized by the introduction of two prolines (S-2P) (Fig. 1d), but immunization with 3M-052 and alum alone did not (Extended Data Fig. 3a, b). Boosting once maximally increased SARS-CoV-2 binding IgG titres (Fig. 1d). ACE2 competitive-binding assays demonstrated the presence of ACE2-binding-site antibodies in the serum of vaccinated macaques (Fig. 1e). Similarly, plasma antibodies blocked the binding of the ACE2-binding-site-focused, RBD-neutralizing antibody DH1041 (Fig. 1e). We assessed the vaccine induction of neutralizing antibodies against a SARS-CoV-2 pseudovirus with an aspartic acid-to-glycine substitution at position 614 (D614G)[32]. Two RBD–scNP immunizations induced potent serum neutralizing antibodies, with ID_{50} neutralization titres that ranged from 21,292 to 162,603 (Fig. 1f, g). We compared these neutralizing antibody titres to those elicited by cynomolgus macaques that were immunized twice with 50 μg of nucleoside-modified mRNA encapsulated in lipid nanoparticles that encodes transmembrane S-2P (S-2P mRNA-LNP). S-2P mRNA-LNP is analogous to COVID-19 vaccines that have been authorized for emergency use (Extended Data Fig. 1f). The serum neutralization titres against SARS-CoV-2 D614G pseudovirus that were elicited by RBD–scNP immunization were significantly higher than titres that were elicited by two immunizations with S-2P mRNA-LNP[33,34] (group geometric mean ID_{50} of 47,216 and 6,469, respectively; $P = 0.0079$ exact Wilcoxon test, $n = 5$ macaques for each vaccine) (Fig. 1i). When compared to natural human infection, RBD–scNP vaccination elicited higher ID_{50} neutralization titres (Fig. 1j). RBD–scNP adjuvanted with 3M-052 and alum therefore elicits significantly higher neutralizing titres in macaques, compared to current vaccine platforms or natural human infection (Fig. 1i, j).

The SARS-CoV-2 variant B.1.1.7 is spreading globally, and has previously been suggested to have higher infectivity than the Wuhan-Hu-1 strain[35,36]. B.1.351-lineage viruses are widespread in the Republic of South Africa[36–38] and—along with the P.1 variant—are of concern owing to their neutralization-resistant phenotype, which is mediated by K417N, E484K and N501Y substitutions in the RBD[39]. Each of these mutations is distal to the cross-nAb DH1047 binding site (owing to its long HCDR3 domain that is used to contact the RBD); however, the E484K substitution is within the binding site of the RBD neutralizing antibody DH1041[15] (Fig. 2a, b). DH1041 binding to the SARS-CoV-2 RBD was therefore knocked out by the E484K substitution, but DH1047 binding to the RBD was unaffected by the K417N, E484K or N501Y substitutions (Fig. 2c, d, Extended Data Fig. 3).

We determined whether immunization with RBD–scNP or S-2P mRNA-LNP elicited neutralizing antibodies against these particular SARS-CoV-2 variants. Serum from macaques vaccinated with RBD–scNP potently neutralized a pseudovirus bearing the D614G spike or the B.1.1.7 spike (Fig. 2d, e). Similarly, S-2P mRNA-LNP immunization elicited equivalent titres of neutralizing antibodies against the B.1.1.7 and D614G variants, although titres were lower than with RBD–scNP immunization (Fig. 2d, e). Serum from macaque immunized with RBD–scNP or S-2P mRNA-LNP neutralized SARS-CoV-2 WA-1, B.1.351 and P.1 pseudoviruses, with 80% inhibitory reciprocal serum dilution

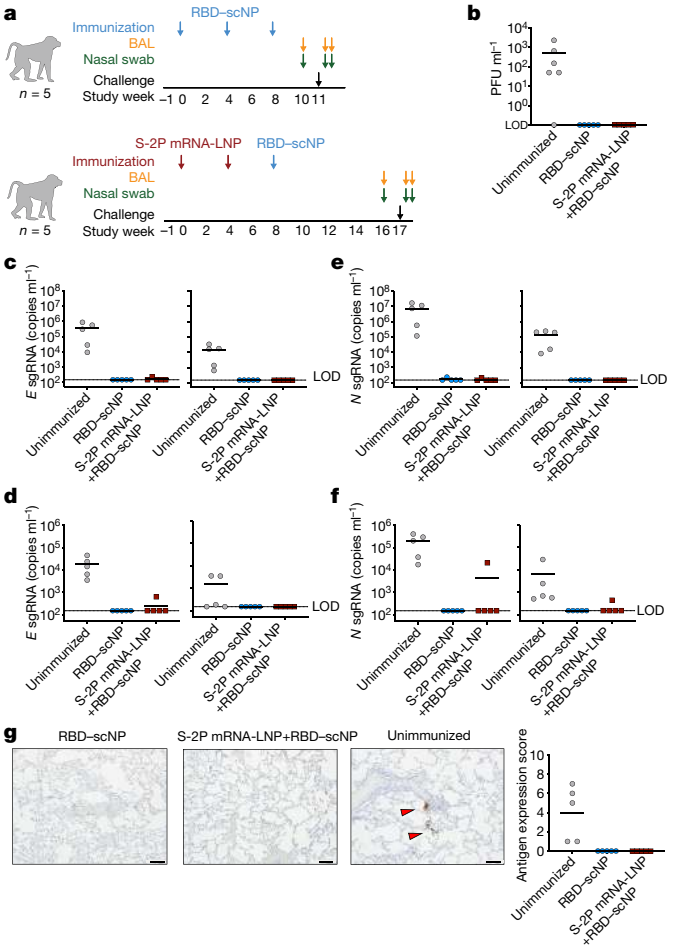

Fig. 4 | RBD–scNP vaccination alone or as a boost can prevent virus replication in the upper and lower respiratory tract after intranasal and intratracheal SARS-CoV-2 challenge in macaques. a, Study design for intranasal and intratracheal challenge of macaques with SARS-CoV-2. Blue and burgundy arrows indicate the time points for RBD–scNP and S-2P mRNA-LNP immunizations, respectively. **b**, Infectious virus in macaque BAL fluid two days after challenge. LOD, limit of detection. **c**–**f**, Quantification of viral *E* gene (**c**, **d**) or *N* gene (**e**, **f**) sgRNA in unimmunized (grey) and RBD–scNP-immunized (blue) macaques, and in macaques with a S-2P mRNA-LNP prime and RBD–scNP boost (burgundy). sgRNA in nasal swabs (**c**, **e**) and BAL fluid (**d**, **f**) was quantified two (left panels) and four (right panels) days after challenge. LOD for the assay is 150 copies per ml. Symbols and bars represent individual macaques and group mean, respectively. **g** Nucleocapsid immunohistochemistry of lung tissue sections at seven days after challenge. Left, representative image from 1 macaque from each group of 5 macaques is shown. Red arrows indicate site of antigen positivity. All images are shown at 10× magnification. Scale bars, 100 μm. Right, quantification of lung viral antigen positivity. In each panel, symbols represent individual macaques (group mean is shown as a black horizontal bar).

(ID_{80}) titres being more potent for the RBD–scNP group (Fig. 2f–i). On average, the neutralization titres in the RBD–scNP group decreased by threefold against the B.1.351 or P.1 variants, whereas those of the S-2P mRNA-LNP group decreased by sixfold for B.1.351 and tenfold for P.1 (on the basis of ID_{50} titres) (Fig. 2g, i). Additionally, we observed that plasma IgG binding to SARS-CoV-2 spike after RBD–scNP and S-2P mRNA-LNP immunization was unaffected by mutations that have been observed in SARS-CoV-2 from Danish minks, as well as in the B.1.351, P.1 and B.1.1.7 strains[36,37,40] (Extended Data Fig. 3). In summary, both of the vaccines we tested elicited neutralizing antibodies that were

unaffected by the mutations in the B.1.1.7 strain. However, neutralizing antibodies elicited by RBD–scNP more potently neutralized the B.1.351 and P.1 virus strains than did neutralizing antibodies elicited with S-2P mRNA-LNP immunization.

SARS-related coronaviruses that circulate in humans and animals remain a threat for future outbreaks[12,41,42]. We therefore examined the neutralization of SARS-CoV, the SARS-related group-2b bat coronavirus WIV-1 and the SARS-related bat coronavirus SHC014 by immune sera from macaques vaccinated with the RBD–scNP, S-2P mRNA-LNP or mRNA-LNP encoding monomeric RBD (RBD mRNA-LNP)[6,9,41,42] (Extended Data Fig. 1e–g). After two immunizations, RBD–scNP, S-2P mRNA-LNP and RBD mRNA-LNP elicited neutralizing antibodies against SARS-CoV, WIV-1 and SHC014 (Fig. 3a, Extended Data Fig. 4). Neutralization was more potent for replication-competent SARS-CoV-2 virus compared to these three SARS-related viruses (Fig. 3a, Extended Data Fig. 4), and neutralization titres varied up to fourfold within the RBD–scNP group (Extended Data Fig. 4). Overall, RBD–scNP immunization elicited the highest neutralization titres (Fig. 3a, Extended Data Fig. 4). Modest increases in neutralization potency were gained by boosting a third time with RBD–scNP (Fig. 3b). Moreover, RBD–scNP immunization elicited cross-reactive plasma IgG against the spike proteins of SARS-CoV-2 and SARS-CoV, as well as those of the bat coronaviruses RaTG13 and SHC014 and the pangolin coronavirus GXP4L (Fig. 3c, Extended Data Fig. 5a, c). Binding antibody titres were high for these spike proteins, even in instances in which neutralization titres were low; this suggests that non-neutralizing antibodies contributed to binding titres. RBD–scNP-immune plasma IgG did not bind the spike protein from the four endemic human coronaviruses or MERS-CoV (Extended Data Fig. 5a, c). The lack of binding by plasma IgG to spike ectodomains of these latter five coronaviruses is consistent with RBD-sequence divergence among group 1, 2a, 2b and 2c coronaviruses (Fig. 3f, Extended Data Figs. 6, 7). The SARS-CoV-2 spike induced cross-nAbs against several group-2b SARS-related betacoronaviruses, with the highest titres being induced by RBD–scNP.

Immune sera from RBD–scNP-immunized macaques exhibited a cross-neutralizing profile similar to that of the cross-nAb DH1047. DH1047 bound with <0.02 nM affinity to monomeric SARS-CoV-2 RBD (Extended Data Fig. 5b), and bound the RBD–scNP (Fig. 1b). The cross-reactive DH1047 epitope is adjacent to the N terminus of the ACE2-binding site, which distinguishes the DH1047 antibody from dominant ACE2-binding- site-focused neutralizing antibodies such as DH1041[15] (Fig. 3d), and the DH1047 epitope has high group-2b sequence conservation (Fig. 3e). Overall RBD sequences within betacoronavirus groups are more conserved than sequences from different groups (Fig. 3f, Extended Data Figs. 6, 7). We determined the presence of DH1047-like antibodies using DH1047 blocking assays. Plasma from all RBD–scNP-immunized macaques blocked the binding of ACE2 and DH1047 to SARS-CoV-2 S-2P (Fig. 3g, Extended Data Fig. 5d). The DH1047-blocking antibodies were cross-reactive, as they also potently blocked DH1047 binding to the S-2P of SHC014 (Fig. 3g). RBD–scNP immunization of macaques elicited higher magnitudes of DH1047-blocking antibodies than did S-2P mRNA-LNP; these magnitudes were also higher than those elicited by immunization of humans with the Pfizer BNT162b2 vaccine or SARS-CoV-2 infection in humans (Fig. 3h, Extended Data Fig. 5d). ACE2 blocking was high in all groups (Fig. 3h). Whereas 5 out of 5 RBD–scNP-vaccinated macaques exhibited potent DH1047 serum blocking activity, 3 out of 4 immunized humans and 9 out of 22 humans who had recovered from COVID-19 had detectable serum DH1047 blocking activity (Fig. 3h). The DH1047-like antibody response was therefore weak and subdominant in naturally infected or immunized humans and S-2P mRNA-LNP-immunized macaques, but was a dominant macaque antibody response to RBD–scNP vaccination.

To determine vaccine protection against coronavirus infection, we challenged RBD–scNP-vaccinated or S-2P mRNA-LNP-primed and RBD–scNP-boosted macaques with 10^5 plaque-forming units of SARS-CoV-2 virus via the intratracheal and intranasal routes, after their last boost (Fig. 4a). Neutralizing antibodies were detectable in all macaques at two weeks after the final immunization (Fig. 3b, Extended Data Fig. 4b, c). We collected bronchoalveolar lavage (BAL) fluid two days after the challenge (Fig. 4a), and detected infectious SARS-CoV-2 in BAL fluid from 5 out of 6 unimmunized macaques, but none of the RBD–scNP or S-2P mRNA-LNP and RBD–scNP-immunized macaques (Fig. 4b). We quantified SARS-CoV-2 replication as the number of copies of envelope (*E*) and nucleocapsid (*N*) subgenomic RNA (sgRNA) in fluid from nasal swabs and BAL at two and four days after challenge (Fig. 4a). At two days after challenge, unimmunized macaques had an average of 1.3×10^5 and 1.2×10^4 copies per ml of *E* sgRNA in the nasal swab and BAL fluids, respectively (Fig. 4c, d). By contrast, all of the RBD–scNP-vaccinated macaques, and 4 out of 5 macaques vaccinated with S-2P mRNA-LNP and RBD–scNP, had undetectable levels of *E* sgRNA in the upper and lower respiratory tract (Fig. 4c, d). We sampled macaques again two days later, and found no detectable *E* sgRNA in the BAL or nasal swab samples from any of the vaccinated macaques (Fig. 4b, c). Similarly, 4 out of 5 RBD–scNP-vaccinated macaques had undetectable *N* sgRNA in BAL and nasal swab fluid; the exception had 234 copies per ml of *N* sgRNA, which was detected on day 2 in nasal swab fluid (Fig. 4e, f). Virus replication was undetectable in this macaque by the fourth day after challenge (Fig. 4e). Additionally, all but one of the macaques immunized with S-2P mRNA-LNP and RBD–scNP had undetectable *N* sgRNA in BAL or nasal swab samples (Fig. 4e,f). Moreover, we did not detect SARS-CoV-2 nucleocapsid antigen in the lung tissue of any of the vaccinated macaques, but detected this antigen in all of the control macaques (Fig. 4g, Extended Data Fig. 8). Haematoxylin and eosin staining of lung tissue showed a reduction in inflammation in immunized macaques compared to control macaques (Extended Data Fig. 8, Extended Data Table 1).

Finally, when possible, we examined mucosal immunity to SARS-CoV-2 both before and after SARS-CoV-2 challenge (Extended Data Fig. 9). IgG from concentrated BAL bound to spike and blocked ACE2, DH1041 and DH1047 binding to spike (Extended Data Fig. 9b–d). Each response was higher in the BAL from macaques immunized three times with RBD–scNP, compared to macaques immunized two times with S-2P mRNA-LNP and boosted once with RBD–scNP (although the BAL was collected from each group at different time points). Unconcentrated nasal wash samples from macaques immunized with either RBD–scNP or a S-2P mRNA-LNP prime and RBD–scNP boost showed similar low levels of spike-binding IgG after challenge (Extended Data Fig. 9e). Nonetheless, RBD–scNP immunization elicited RBD-specific mucosal antibodies.

As three coronavirus epidemics have occurred in the past 20 years, there is a need to develop vaccines that are effective against all coronaviruses before the next pandemic[25]. The epitopes of betacoronavirus cross-nAbs (such as DH1047) provide clear targets for vaccines that aim to protect against multiple coronaviruses[13–15,43]. We have shown that immunization of macaques with RBD–scNP adjuvanted with 3M-052 and—to a lesser extent—S-2P mRNA-LNP induces cross-nAbs against multiple SARS-related human and bat betacoronaviruses. These results demonstrate that SARS-CoV-2 vaccination with either the RBD–scNP or S-2P mRNA-LNP vaccines (the latter of which are similar to vaccines that have already been authorized for use in humans) will probably elicit cross-nAbs, and have the potential to prevent future spillovers of group-2b betacoronaviruses from bats to humans[12,26].

The emergence of neutralization-resistant and highly infectious variants of SARS-CoV-2 continues to be a concern for vaccine efficacy. The RBD–scNP and S-2P mRNA-LNP immunizations elicited SARS-CoV-2 neutralizing antibodies against the D614G, B.1.1.7, P.1 and B.1.351 strains of SARS-CoV-2. The neutralizing antibodies elicited by RBD–scNP and S-2P mRNA-LNP were of different specificities, as RBD–scNP-induced neutralizing antibodies showed a smaller reduction in neutralization potency across the different variants compared to S-2P mRNA-LNP

immune sera. Our results are consistent with the previous demonstration that current COVID-19 vaccines have reduced efficacy against the B.1.351 SARS-CoV-2 variant[39,44–48].

The RBD–scNP vaccine is a promising platform for the development of vaccines that target multiple coronaviruses for the following reasons. The RBD–scNP vaccine induced apparent sterilizing immunity in the upper respiratory tract, which has not been routinely achieved with SARS-CoV-2 vaccination in macaques[49,50]. Additionally, the high neutralization titres achieved by RBD–scNP vaccination bode well for an extended duration of protection. Despite the induction of high levels of antibody, we observed no evidence of increased immunopathology, inflammatory cytokines or virus replication indicative of vaccine-elicited antibody-dependent enhancement. This lack of in vivo infection enhancement is consistent with previous studies using SARS-CoV-2 monoclonal antibodies[15]. 3M-052 adsorbed to alum is in clinical testing (NCT04177355), which generates a potential translational pathway for RBD–scNP adjuvanted with 3M-052. The RBD–scNP vaccine represents a platform for inducing high titres of protective antibodies against current human coronaviruses and their variants, and for producing vaccines that could prevent, rapidly temper or extinguish the next spillover of a coronavirus into humans.

Online content

Any methods, additional references, Nature Research reporting summaries, source data, extended data, supplementary information, acknowledgements, peer review information; details of author contributions and competing interests; and statements of data and code availability are available at https://doi.org/10.1038/s41586-021-03594-0.

1. Wang, C., Horby, P. W., Hayden, F. G. & Gao, G. F. A novel coronavirus outbreak of global health concern. *Lancet* **395**, 470–473 (2020).
2. Zaki, A. M., van Boheemen, S., Bestebroer, T. M., Osterhaus, A. D. & Fouchier, R. A. Isolation of a novel coronavirus from a man with pneumonia in Saudi Arabia. *N. Engl. J. Med.* **367**, 1814–1820 (2012).
3. Zhong, N. S. et al. Epidemiology and cause of severe acute respiratory syndrome (SARS) in Guangdong, People's Republic of China, in February, 2003. *Lancet* **362**, 1353–1358 (2003).
4. Zhu, N. et al. A novel coronavirus from patients with pneumonia in China, 2019. *N. Engl. J. Med.* **382**, 727–733 (2020).
5. Zhou, P. et al. A pneumonia outbreak associated with a new coronavirus of probable bat origin. *Nature* **579**, 270–273 (2020).
6. Li, W. et al. Bats are natural reservoirs of SARS-like coronaviruses. *Science* **310**, 676–679 (2005).
7. Olival, K. J. et al. Host and viral traits predict zoonotic spillover from mammals. *Nature* **546**, 646–650 (2017).
8. Sabir, J. S. et al. Co-circulation of three camel coronavirus species and recombination of MERS-CoVs in Saudi Arabia. *Science* **351**, 81–84 (2016).
9. Ge, X. Y. et al. Isolation and characterization of a bat SARS-like coronavirus that uses the ACE2 receptor. *Nature* **503**, 535–538 (2013).
10. Guan, Y. et al. Isolation and characterization of viruses related to the SARS coronavirus from animals in southern China. *Science* **302**, 276–278 (2003).
11. Xiao, K. et al. Isolation of SARS-CoV-2-related coronavirus from Malayan pangolins. *Nature* **583**, 286–289 (2020).
12. Menachery, V. D., Graham, R. L. & Baric, R. S. Jumping species–a mechanism for coronavirus persistence and survival. *Curr. Opin. Virol.* **23**, 1–7 (2017).
13. Pinto, D. et al. Cross-neutralization of SARS-CoV-2 by a human monoclonal SARS-CoV antibody. *Nature* **583**, 290–295 (2020).
14. Wec, A. Z. et al. Broad neutralization of SARS-related viruses by human monoclonal antibodies. *Science* **369**, 731–736 (2020).
15. Li, D. et al. The functions of SARS-CoV-2 neutralizing and infection-enhancing antibodies in vitro and in mice and nonhuman primates. Preprint at https://doi.org/10.1101/2020.12.31.424729 (2021).
16. Shi, R. et al. A human neutralizing antibody targets the receptor-binding site of SARS-CoV-2. *Nature* **584**, 120–124 (2020).
17. Ju, B. et al. Human neutralizing antibodies elicited by SARS-CoV-2 infection. *Nature* **584**, 115–119 (2020).
18. Robbiani, D. F. et al. Convergent antibody responses to SARS-CoV-2 in convalescent individuals. *Nature* **584**, 437–442 (2020).
19. Zost, S. J. et al. Potently neutralizing and protective human antibodies against SARS-CoV-2. *Nature* **584**, 443–449 (2020).
20. Liu, L. et al. Potent neutralizing antibodies against multiple epitopes on SARS-CoV-2 spike. *Nature* **584**, 450–456 (2020).
21. Hansen, J. et al. Studies in humanized mice and convalescent humans yield a SARS-CoV-2 antibody cocktail. *Science* **369**, 1010–1014 (2020).
22. Brouwer, P. J. M. et al. Potent neutralizing antibodies from COVID-19 patients define multiple targets of vulnerability. *Science* **369**, 643–650 (2020).
23. Rogers, T. F. et al. Isolation of potent SARS-CoV-2 neutralizing antibodies and protection from disease in a small animal model. *Science* **369**, 956–963 (2020).
24. Piccoli, L. et al. Mapping neutralizing and immunodominant sites on the SARS-CoV-2 spike receptor-binding domain by structure-guided high-resolution serology. *Cell* **183**, 1024–1042.e21 (2020).
25. Burton, D. R. & Walker, L. M. Rational vaccine design in the time of COVID-19. *Cell Host Microbe* **27**, 695–698 (2020).
26. Cohen, A. A. et al. Mosaic nanoparticles elicit cross-reactive immune responses to zoonotic coronaviruses in mice. *Science* **371**, 735–741 (2021).
27. Ma, X. et al. Nanoparticle vaccines based on the receptor binding domain (RBD) and heptad repeat (HR) of SARS-CoV-2 elicit robust protective immune responses. *Immunity* **53**, 1315–1330.e9 (2020).
28. Bangaru, S. et al. Structural analysis of full-length SARS-CoV-2 spike protein from an advanced vaccine candidate. *Science* **370**, 1089–1094 (2020).
29. Walls, A. C. et al. Elicitation of potent neutralizing antibody responses by designed protein nanoparticle vaccines for SARS-CoV-2. *Cell* **183**, 1367–1382.e17 (2020).
30. Saunders, K. O. et al. Targeted selection of HIV-specific antibody mutations by engineering B cell maturation. *Science* **366**, eaay7199 (2019).
31. Fox, C. B. et al. Adsorption of a synthetic TLR7/8 ligand to aluminum oxyhydroxide for enhanced vaccine adjuvant activity: a formulation approach. *J. Control. Release* **244** (Pt A), 98–107 (2016).
32. Korber, B. et al. Tracking changes in SARS-CoV-2 spike: evidence that D614G increases infectivity of the COVID-19 virus. *Cell* **182**, 812–827.e19 (2020).
33. Baden, L. R. et al. Efficacy and safety of the mRNA-1273 SARS-CoV-2 vaccine. *N. Engl. J. Med.* **384**, 403–416 (2021).
34. Polack, F. P. et al. Safety and efficacy of the BNT162b2 mRNA Covid-19 vaccine. *N. Engl. J. Med.* **383**, 2603–2615 (2020).
35. Galloway, S. E. et al. Emergence of SARS-CoV-2 B.1.1.7 lineage – United States, December 29, 2020–January 12, 2021. *MMWR Morb. Mortal. Wkly. Rep.* **70**, 95–99 (2021).
36. Leung, K., Shum, M. H., Leung, G. M., Lam, T. T. & Wu, J. T. Early transmissibility assessment of the N501Y mutant strains of SARS-CoV-2 in the United Kingdom, October to November 2020. *Euro Surveill.* **26**, 2002106 (2021).
37. Faria, N. R. et al. Genomic characterisation of an emergent SARS-CoV-2 lineage in Manaus: preliminary findings. *Virological* https://virological.org/t/genomic-characterisation-of-an-emergent-sars-cov-2-lineage-in-manaus-preliminary-findings/586 (2021).
38. Tegally, H. et al. Sixteen novel lineages of SARS-CoV-2 in South Africa. *Nat. Med.* **27**, 440–446 (2021).
39. Wibmer, C. K. et al. SARS-CoV-2 501Y.V2 escapes neutralization by South African COVID-19 donor plasma. *Nat. Med.* **27**, 622–625 (2021).
40. Lassaunière, R. et al. SARS-CoV-2 spike mutations arising in Danish mink and their spread to humans. https://files.ssi.dk/Mink-cluster-5-short-report_AFO2 (2021).
41. Menachery, V. D. et al. A SARS-like cluster of circulating bat coronaviruses shows potential for human emergence. *Nat. Med.* **21**, 1508–1513 (2015).
42. Menachery, V. D. et al. SARS-like WIV1-CoV poised for human emergence. *Proc. Natl Acad. Sci. USA* **113**, 3048–3053 (2016).
43. Liu, H. et al. Cross-neutralization of a SARS-CoV-2 antibody to a functionally conserved site is mediated by avidity. *Immunity* **53**, 1272–1280.e5 (2020).
44. Muik, A. et al. Neutralization of SARS-CoV-2 lineage B.1.1.7 pseudovirus by BNT162b2 vaccine-elicited human sera. *Science* **371**, 1152–1153 (2021).
45. Wu, K. et al. mRNA-1273 vaccine induces neutralizing antibodies against spike mutants from global SARS-CoV-2 variants. Preprint at https://doi.org/10.1101/2021.01.25.427948 (2021).
46. Cele, S. et al. Escape of SARS-CoV-2 501Y.V2 variants from neutralization by convalescent plasma. Preprint at https://doi.org/10.1101/2021.01.26.21250224 (2021).
47. Collier, D. et al. Sensitivity of SARS-CoV-2 B.1.1.7 to mRNA vaccine-elicited antibodies. *Nature* **593**, 136–141 (2021).
48. Wang, Z. et al. mRNA vaccine-elicited antibodies to SARS-CoV-2 and circulating variants. *Nature*, **592**, 616–622 (2021).
49. Yu, J. et al. DNA vaccine protection against SARS-CoV-2 in rhesus macaques. *Science* **369**, 806–811 (2020).
50. Mercado, N. B. et al. Single-shot Ad26 vaccine protects against SARS-CoV-2 in rhesus macaques. *Nature* **586**, 583–588 (2020).

Methods

The experiments were not randomized, and only the pathologists were blinded to group treatments during experiments and outcome assessment.

Animals, immunizations, and human samples

Rhesus and cynomolgus macaques were housed and treated in Association for Assessment and Accreditation of Laboratory Animal Care (AAALAC)-accredited institutions. The study protocol and all veterinarian procedures were approved by the Bioqual IACUC per a memorandum of understanding with the Duke IACUC, and were performed based on standard operating procedures. Macaques studied were housed and maintained in an AAALAC-accredited institution in accordance with the principles of the NIH. All studies were carried out in strict accordance with the recommendations in the Guide for the Care and Use of Laboratory Animals of the NIH in BIOQUAL. BIOQUAL is fully accredited by AAALAC and through OLAW, assurance number A-3086. All physical procedures associated with this work were done under anaesthesia to minimize pain and distress, in accordance with the recommendations of the Weatherall report 'The use of non-human primates in research.' Teklad 5038 primate diet was provided once daily by macaque size and weight. The diet was supplemented with fresh fruit and vegetables. Fresh water was given ad libitum. All macaques were maintained in accordance with the Guide for the Care and Use of Laboratory Animals. mRNA-LNP was prepared as previously stated[51,52]. Rhesus macaques (n = 8 macaques) were immunized intramuscularly twice with 50 μg of RBD mRNA-LNP. Cynomolgus macaques (n = 5 macaques) were immunized twice with 50 μg of S-2P mRNA-LNP (encoding the transmembrane spike protein stabilized with K986P and V987P mutations) and boosted once with 100 μg of RBD–scNP adjuvanted with 5 μg of 3M-052 aqueous formulation admixed with 500 μg of alum in PBS. An additional group of cynomolgus macaques (n = 5 macaques) were immunized in the right and left quadriceps with 100 μg of RBD–scNP adjuvanted with 5 μg of 3M-052 aqueous formulation admixed with 500 μg of Alum in PBS[31]. The mixture for immunization consisted of 250 μl of RBD–scNP mixed with 250 μl of 0.02 mg ml^{-1} 3M-052 and 2 mg ml^{-1} alum. Group sizes were selected such that statistical significance could be reached with between group nonparametric statistical comparisons. No other statistical methods were used to predetermine sample size. Macaques were on average 8 or 9 years old and ranged from 2.75 to 8 kg in body weight. Male and female macaques per group were balanced when availability permitted. Studies were performed unblinded. Macaques were evaluated by Bioqual veterinary staff before, during and after immunizations. In the macaques studied, complete blood counts and chemistries were obtained throughout the immunization regimen and no marked abnormalities were noted. Of the 10 cynomolgus macaques, there were no adverse events reported at injection sites. Over the course of the study, two cynomolgus macaques experienced slight weight loss. Two cynomolgus macaques showed a single incidence of poor appetite, with one additional cynomolgus macaque showing poor appetite intermittently throughout the study. Additionally, one macaque presented with an infected lymph node biopsy site that responded to appropriate veterinary treatment. Biospecimens were collected before challenge, and 2 and 4 days after challenge, as previously described[15]. Human samples were obtained with informed consent. All recruitment, sample collection and experimental procedures using human samples have been approved by the Duke Institutional Review Board.

SARS-CoV-2 intranasal and intratracheal challenge

All macaques were challenged at week 11 (3 weeks after last vaccination) through combined intratracheal (3.0 ml) and intranasal (0.5 ml per nostril) inoculation with an infectious dose of 10^5 plaque-forming units (PFU) of SARS-CoV-2 (2019-nCoV/USA-WA1/2020). The stock was generated at BIOQUAL (lot no. 030120-1030, 3.31×10^5 PFU ml^{-1}) from a p4 seed stock obtained from BEI Resources (NR-52281). The stock underwent deep sequencing to confirm homology with the WA1/2020 isolate. Virus was stored at −80 °C before use, thawed by hand and placed immediately on wet ice. Stock was diluted to 2.5×10^4 PFU ml^{-1} in PBS and vortexed gently for 5 s before inoculation. Nasal swabs, BAL, plasma and serum samples were collected seven days before, two days after and four days after challenge. Unimmunized control cynomolgus macaques (n = 5) comprised macaques that had been infused with a 10 mg kg^{-1} of a control antibody (CH65) and then 3 days later challenged with the same challenge dose and stock of SARS-CoV-2 as used in RBD–scNP-immunized macaques or S-2P mRNA-LNP and RBD–scNP-immunized macaques. Protection from SARS-CoV-2 infection was determined by quantitative PCR of SARS-CoV-2 subgenomic E and the more-sensitive N RNA (E or N sgRNA)[39] as stated in 'sgRNA real-time PCR quantification'.

SARS-CoV-2 protein production

The coronavirus ectodomain DNA constructs were synthesized (Genscript), produced and purified as previously described[53]. S-2P was stabilized by the introduction of 2 prolines at amino acid positions 986 and 987. Plasmids encoding S-2P and HexaPro[54] were transiently transfected in FreeStyle 293 cells (Thermo Fisher) using Turbo293 (SpeedBiosystems) or 293Fectin (ThermoFisher). All cells were tested monthly for mycoplasma. The constructs contained an HRV 3C-cleavable C-terminal twinStrepTagII-8×His tag. On day 6, cell-free culture supernatant was generated by centrifugation of the culture and filtering through a 0.8-μm filter. Protein was purified from filtered cell culture supernatants by StrepTactin resin (IBA) and by size-exclusion chromatography using Superose 6 column (GE Healthcare) in 10 mM Tris pH8,150 mM NaCl or 2 mM Tris pH 8, 200 mM NaCl, 0.02% NaN_3. ACE2–Fc was expressed by transient transfection of Freestyle 293-F cells[53]. ACE2–Fc was purified from cell culture supernatant by HiTrap protein A column chromatography and Superdex200 size-exclusion chromatography in 10 mM Tris pH8,150 mM NaCl. SARS-CoV-2 NTD was produced as previously described[55]. SARS-CoV-2 fusion peptide was synthesized (GenScript).

Sortase A conjugation of SARS-CoV-2 RBD to *H. pylori* ferritin nanoparticles

Wuhan strain SARS-CoV-2 RBD was expressed with a sortase A donor sequence LPETGG encoded at its C terminus. C-terminal to the sortase A donor sequence was an HRV-3C cleavage site, 8×His tag and a twin StrepTagII (IBA). The SARS-CoV-2 RBD was expressed in Freestyle 293 cells and purified by StrepTactin affinity chromatography (IBA) and Superdex200 size-exclusion chromatography as stated in 'SARS-CoV-2 protein production'. *Helicobacter pylori* ferritin particles were expressed with a pentaglycine sortase A acceptor sequence encoded at its N terminus of each subunit. For affinity purification of ferritin particles, 6×His tags were appended C-terminal to a HRV3C cleavage site. Ferritin particles with a sortase A N-terminal tag were buffer exchanged into 50 mM Tris, 150 mM NaCl, 5 mM $CaCl_2$, pH 7.5. Then, 180 μM SARS-CoV-2 RBD was mixed with 120 μM of ferritin subunits and incubated with 100 μM of sortase A overnight at room temperature. Following incubation, conjugated particles were isolated from free ferritin or free RBD by size-exclusion chromatography using a Superose6 16/60 column.

Biolayer interferometry binding assays

Binding was measured using an OctetRed 96 (ForteBio). Anti-human IgG capture (AHC) sensor tips (Forte Bio) were hydrated for at least 10 min in PBS. ACE2 and monoclonal antibodies were diluted to 20 μg ml^{-1} in PBS and placed in black 96-well assay plate. The influenza antibody CH65 was used as the background reference antibody. The RBD nanoparticle was diluted to 50 μg ml^{-1} in PBS and added to the assay plate. Sensor tips were loaded with antibody for 120 s. Subsequently, the sensor tips

were washed for 60 s in PBS to removed unbound antibody. The sensor tips were incubated in a fresh well of PBS to establish baseline reading before being dipped into RBD–scNP to allow association for 400 s. To measure dissociation of the antibody–RBD–scNP complex, the tip was incubated in PBS for 600 s. At the end of dissociation, the tip was ejected and a new tip was attached to load another antibody. The data were analysed with Data Analysis HT v.12 (ForteBio). Background binding observed with CH65 was subtracted from all values. All binding curves were aligned to the start of association. The binding response at the end of the 400-s association phase was plotted in GraphPad Prism v.9.0.

Surface plasmon resonance assays

Surface plasmon resonance measurements of DH1047 antigen binding fragment (Fab) binding to monomeric SARS-CoV-2 RBD proteins were performed in HBS-EP+ running buffer using a Biacore S200 instrument (Cytiva). Assays were performed in the DHVI BIA Core Facility. The RBD was first captured via its twin-StrepTagII onto a Series S Streptavidin chip to a level of 300–400 resonance units. The antibody Fabs were injected at 0.5 to 500 nM over the captured spike proteins using the single cycle kinetics injection mode at a flow rate of 50 µl min^{-1}. Fab association occurred for 180 s followed by a dissociation of 360 s after the end of the association phase. At the end of the dissociation phase, the RBD was regenerated with a 30-s injection of glycine pH 1.5. Binding values were analysed with Biacore S200 Evaluation software (Cytiva). References included blank streptavidin surface along with blank buffer binding and was subtracted from DH1047 values to account for signal drift and non-specific protein binding. A 1:1 Langmuir model with a local R_{max} was used for curve fitting. Binding rates and constants were derived from the curve. Representative results from two independent experiments are shown.

BAL plaque assay

SARS-CoV-2 plaque assays were performed in the Duke Regional Biocontainment biosafery level 3 (BSL3) Laboratory as previously described[56]. Serial dilutions of BAL fluid were incubated with Vero E6 cells in a standard plaque assay[57,58]. BAL and cells were incubated at 37 °C and 5% CO_2 for 1 h. At the end of the incubation, 1 ml of a viscous overlay (1:1 2× DMEM and 1.2% methylcellulose) was added to each well. Plates are incubated for four days. After fixation, staining and washing, plates were dried and plaques from each dilution of BAL sample were counted. Data are reported as PFU ml^{-1} of BAL fluid. Samples were collected in virus transport medium from six unimmunized, SARS-CoV-2-challenged macaques for comparison to vaccinated macaques.

SARS-CoV-2 pseudovirus neutralization

For SARS-CoV-2(D614G) and SARS-CoV-2 B.1.1.7 pseudovirus neutralization assays, neutralization of SARS-CoV-2 spike-pseudotyped virus was performed by adapting a previously described infection assay with lentiviral vectors and infection in 293T/ACE2.MF (the cell line was provided by M. Farzan and H. Mu at Scripps). Cells were maintained in DMEM containing 10% FBS and 50 µg ml^{-1} gentamicin. An expression plasmid encoding codon-optimized full-length spike of the Wuhan-1 strain (VRC7480) was provided by B. Graham and K. Corbett at the Vaccine Research Center, National Institutes of Health. The D614G substitution was introduced into VRC7480 by site-directed mutagenesis using the QuikChange Lightning Site-Directed Mutagenesis Kit from Agilent Technologies (210518). The mutation was confirmed by full-length spike gene sequencing. Pseudovirions were produced in HEK 293T/17 cells (ATCC, CRL-11268) by transfection using Fugene 6 (Promega, E2692). Pseudovirions for infection of 293T cells expressing ACE2 were produced by co-transfection with a lentiviral backbone (pCMV ΔR8.2) and firefly luciferase reporter gene (pHR' CMV Luc)[59]. Culture supernatants from transfections were clarified of cells by low-speed centrifugation and filtration (0.45-µm filter) and stored in 1 ml aliquots at −80 °C.

For neutralization assays in 293T cells expressing ACE2, a pretitrated dose of virus was incubated with 8 serial threefold or fivefold dilutions of monoclonal antibodies in duplicate in a total volume of 150 µl for 1 h at 37 °C in 96-well flat-bottom poly-L-lysine-coated culture plates (Corning Biocoat). SARS-CoV-2 RBD neutralizing antibody DH1043 spiked into normal human serum was used as a positive control. Cells were suspended using TrypLE express enzyme solution (Thermo Fisher Scientific) and immediately added to all wells (10,000 cells in 100 µl of growth medium per well). One set of eight control wells received cells + virus (virus control) and another set of eight wells received cells only (background control). After 66–72 h of incubation, medium was removed by gentle aspiration and 30 µl of Promega 1× lysis buffer was added to all wells. After a 10-min incubation at room temperature, 100 µl of Bright-Glo luciferase reagent was added to all wells. After 1–2 min, 110 µl of the cell lysate was transferred to a black/white plate (Perkin-Elmer). Luminescence was measured using a PerkinElmer Life Sciences, Model Victor2 luminometer.

To make WA-1, P.1 and B.1.351 SARS-CoV-2 pseudoviruses, human codon-optimized cDNA encoding SARS-CoV-2 spike glycoproteins of various strains were synthesized by GenScript and cloned into eukaryotic cell expression vector pcDNA 3.1 between the BamHI and XhoI sites. Pseudovirions were produced by co-transfection of Lenti-X 293T cells with psPAX2(gag/pol), pTrip-luc lentiviral vector and pcDNA 3.1 SARS-CoV-2-spike-deltaC19, using Lipofectamine 3000. The supernatants were collected at 48 h after transfection and filtered through 0.45-µm membranes and titrated using HEK293T cells that express ACE2 and TMPRSS2 protein (293-ACE2-TMPRSS2 cells).

For the neutralization assay, 50 µl of SARS-CoV-2 spike pseudovirions were pre-incubated with an equal volume of medium containing serum at varying dilutions at room temperature for 1 h, then virus-antibody mixtures were added to 293T cells expressing ACE2 (WA-1 and B.1.351 assays) or 293-ACE2-TMPRSS2 (WA-1 and P.1 assays) cells in a 96-well plate. After a 3-h incubation, the inoculum was replaced with fresh medium. Cells were lysed 24 h later, and luciferase activity was measured using luciferin. Controls included cell-only control, virus without any antibody control and positive control sera. Neutralization titres are the serum dilution (ID_{50} or ID_{80}) at which relative luminescence units (RLU) were reduced by 50% or 80%, respectively, compared to virus control wells after subtraction of background RLUs.

Live virus neutralization assays

Full-length SARS-CoV-2, SARS-CoV, WIV-1 and RsSHC014 viruses were designed to express nanoluciferase (nLuc) and were recovered via reverse genetics as previously described[60–62]. Virus titres were measured in Vero E6 USAMRIID cells, as defined by PFU ml^{-1}, in a 6-well plate format in quadruplicate biological replicates for accuracy. For the 96-well neutralization assay, Vero E6 USAMRID cells were plated at 20,000 cells per well the day previously in clear-bottom black-walled plates. Cells were inspected to ensure confluency on the day of assay. Serum samples were tested at a starting dilution of 1:20 and were serially diluted threefold up to nine dilution spots. Serially diluted serum samples were mixed in equal volume with diluted virus. Antibody–virus and virus-only mixtures were then incubated at 37 °C with 5% CO_2 for 1 h. Following incubation, serially diluted sera and virus-only controls were added in duplicate to the cells at 75 PFU at 37 °C with 5% CO_2. After 24 h, cells were lysed, and luciferase activity was measured via Nano-Glo Luciferase Assay System (Promega) according to the manufacturer specifications. Luminescence was measured by a Spectramax M3 plate reader (Molecular Devices). Virus neutralization titres were defined as the sample dilution at which a 50% reduction in RLU was observed relative to the average of the virus control wells. Prebleed or unimmunized control macaque values were subtracted from WIV-1 neutralization titres, but all other viruses were not background-subtracted.

Biocontainment and biosafety

All work was performed with approved standard operating procedures for SARS-CoV-2 in a BSL3 facility conforming to requirements recommended in the Microbiological and Biomedical Laboratories, by the US Department of Health and Human Service, the US Public Health Service, and the US Center for Disease Control and Prevention and the NIH.

Plasma and mucosal IgG blocking of ACE2 binding

For ACE2 blocking assays, plates were coated with 2 μg ml^{-1} recombinant ACE2 protein, then washed and blocked with 3% BSA in 1× PBS. While assay plates blocked, purified antibodies were diluted as stated in 'Plasma and mucosal IgG ELISA binding assays', only in 1% BSA with 0.05% Tween-20. In a separate dilution plate, S-2P was mixed with the antibodies at a final concentration equal to the half-maximal effective concentration at which spike binds to ACE2 protein. The mixture was allowed to incubate at room temperature for 1 h. Blocked assay plates were then washed and the antibody–spike mixture was added to the assay plates for a period of 1 h at room temperature. Plates were washed and a polyclonal rabbit serum against the same spike protein (S-2P expressed in Freestyle 293-F cells) was added for 1 h, washed and detected with goat anti rabbit-HRP (Abcam, ab97080) followed by TMB substrate. The extent to which antibodies were able to block the binding of the spike protein to ACE2 was determined by comparing the optical density (OD) of antibody samples at 450 nm to the OD of samples containing spike protein only with no antibody. The following formula was used to calculate the percentage of blocking: blocking % = (100 − (OD sample/OD of spike only) × 100).

Plasma and mucosal IgG blocking of RBD monoclonal antibody binding

Blocking assays for DH1041 and DH1047 were performed as stated in 'Plasma and mucosal IgG blocking of ACE2 binding', except plates were coated with either DH1041 or DH1047 instead of ACE2.

Plasma and mucosal IgG ELISA binding assays

For ELISA binding assays of coronavirus spike antibodies, the antigen panel included SARS-CoV-2 spike S1 + S2 ECD (SINO, 40589-V08B1), SARS-CoV-2 S-2P[53], SARS-CoV-2 spike RBD from mammalian cell 293 (SINO, 40592- V08H), SARS-CoV-2 spike NTD–biotin, SARS-CoV-2 fusion peptide (FP), SARS-CoV spike protein delta (BEI, NR-722), SARS-CoV WH20 spike RBD (SINO, 40150-V08B2), SARS-CoV RBD, MERS-CoV spike S1 + S2 (SINO, 40069-V08B), pangolin GXP4L S-2P, Bat CoV-RaTG13 S-2P, and bat CoV-SHC014 S-2P.

For binding ELISA, 384-well ELISA plates were coated with 2 μg ml^{-1} of antigens in 0.1 M sodium bicarbonate overnight at 4 °C. Plates were washed with PBS + 0.05% Tween 20 and blocked with assay diluent (PBS containing 4% (w/v) whey protein, 15% normal goat serum, 0.5% Tween-20, and 0.05% sodium azide) at room temperature for 1 h. Plasma or mucosal fluid were serially diluted threefold in superblock starting at a 1:30 dilution. Nasal fluid was started from neat and diluted 1:30, whereas BAL fluid was concentrated tenfold. To concentrate BAL, individual BAL aliquots from the same macaque and same time point were pooled in 3-kDa MWCO ultrafiltration tubes (Sartorious, VS2091). Pooled BAL was concentrated by centrifugation at 3,500 rpm for 30 min or until volume was reduced by a factor of 10. The pool was then aliquoted and frozen at −80 °C until its use in an assay. Purified monoclonal antibody samples were diluted to 100 μg ml^{-1} and then serially diluted threefold in assay diluent. Samples were added to the antigen-coated plates, and incubated for 1 h, followed by washes with PBS-0.1% Tween 20. HRP-conjugated goat anti-human IgG secondary antibody or mouse anti-rhesus IgG secondary antibody (SouthernBiotech, 2040-05) was diluted to 1:10,000 and incubated at room temperature for 1 h. These plates were washed four times and developed with tetramethylbenzidine substrate (SureBlue Reserve-KPL). The reaction was stopped with 1 M HCl, and OD at 450 nm was determined.

sgRNA real-time PCR quantification

SARS-CoV-2 *E* gene and *N* gene subgenomic mRNAs were measured by one-step RT–qPCR adapted from previously described methods[63,64]. *E* and *N* genes were cloned into pCDNA3.1 and used as in vitro transcription templates. In vitro transcribed RNA was generated with the MEGAscript T7 Transcription Kit (ThermoFisher, AM1334) and purified with MEGAclear Transcription Clean-Up Kit (ThermoFisher, AM1908). Pure RNA was quantified and used as standards for qPCR. RNA extracted from animal samples was quantified using TaqMan Fast Virus 1-Step Master Mix (ThermoFisher, 4444432) and custom primers and probes targeting the *E* gene sgRNA (forward primer, 5′-CGATCTCTTGTAGATCTGTTCTCE-3′; reverse primer, 5′-ATATTGCAGCAGTACGCACACA-3′; probe, 5′-FAM-ACACTAGCCATCCTTACTGCGCTTCG-BHQ1-3′) or the *N* gene sgRNA (forward primer, 5′-CGATCTCTTGTAGATCTGTTCTC-3′; reverse primer, 5′-GGTGAACCAAGACGCAGTAT-3′; probe, 5′-FAM-TAACCA GAATGGAGAACGCAGTG GG-BHQ1-3′). A QuantStudio 3 Real-Time PCR System (Applied Biosystems) or a StepOnePlus Real-Time PCR System (Applied Biosystems) was used for real-time PCR reactions. Cycle conditions were as follows: reverse transcription at 50 °C for 5 min, initial denaturation at 95 °C for 20 s, and 40 cycles of denaturation–annealing–extension at 95 °C for 15 s and 60 °C for 30 s. Standard curves were used to calculate *E* or *N* sgRNA in copies per ml. The LOD for both *E* and *N* sgRNA assays were 12.5 copies per reaction or 150 copies per ml of BAL, nasal swab or nasal wash.

Recombinant IgG production

Expi293-F cells were diluted to 2.5 × 10^6 cells per ml on the day of transfection. Cells were co-transfected with expifectamine and heavy and light chain expression plasmids. Enhancers were added 16 h after transfection. On day 5, the cell culture was cleared of cells by centrifugation, filtered and incubated with protein A beads overnight. The next day, the protein A resin was washed with Tris buffered saline and then added to a 25-ml column. The resin was washed again and then glacial acetic acid was used to elute antibody off of the protein A resin. The pH of the solution was neutralized with 1 M Tris pH 8. The antibody was buffer-exchanged into 25 mM sodium citrate pH 6 supplemented with 150 mM NaCl, 0.2-μm filtered and frozen at −80 °C.

Negative-stain electron microscopy

The RBD nanoparticle protein at about 1–5 mg ml^{-1} concentration that had been flash-frozen and stored at −80 °C was thawed in an aluminium block at 37 °C for 5 min; then 1–4 μl of RBD nanoparticle was diluted to a final concentration of 0.1 mg ml^{-1} into room-temperature buffer containing 150 mM NaCl, 20 mM HEPES pH 7.4, 5% glycerol and 7.5 mM glutaraldehyde. After 5 min of cross-linking, excess glutaraldehyde was quenched by adding sufficient 1 M Tris pH 7.4 stock to give a final concentration of 75 mM Tris and incubated for 5 min. For negative stain, carbon-coated grids (EMS, CF300-cu-UL) were glow-discharged for 20 s at 15 mA, after which a 5-μl drop of quenched sample was incubated on the grid for 10–15 s, blotted and then stained with 2% uranyl formate. After air drying, grids were imaged with a Philips EM420 electron microscope operated at 120 kV, at 82,000× magnification and images captured with a 2k × 2k CCD camera at a pixel size of 4.02 Å.

Processing of negative-stain images

The RELION 3.0 program was used for all negative-stain image processing. Images were imported, CTF-corrected with CTFFIND and particles were picked using a nanoparticle template from previous 2D class averages of nanoparticles alone. Extracted particle stacks were subjected

to 2 or 3 rounds of 2D class averaging and selection to discard junk particles and background picks.

Betacoronavirus sequence analysis

Heat maps of amino acid sequence similarity were computed for a representative set of betacoronaviruses using the ComplexHeatmap package in R. In brief, 1,408 betacoronavirus sequences were retrieved from NCBI GenBank, aligned to the Wuhan-1 spike protein sequence and trimmed to the aligned region. The 1,408 spike sequences were then clustered using USEARCH[65] with a sequence identity threshold of 0.90, resulting in 52 clusters. We sampled one sequence from each cluster to generate a representative set of sequences. Five betacoronavirus sequences of interest not originally included in the clustered set were added: SARS-CoV-2, GXP4L, bat coronavirus RaTG13, bat coronavirus SHC014 and bat coronavirus WIV-1. This resulted in a set of 57 representative spike sequences. Pairs of spike amino acid sequences were aligned using a global alignment and the BLOSUM62 scoring matrix. For RBD and NTD domain alignments, spike sequences were aligned to the Wuhan-1 spike protein RBD region (residues 330–521) and NTD region (residues 27–292), respectively, and trimmed to the aligned region. Phylogenetic tree construction of RBD sequences was performed with Geneious Prime 2020.1.2 using the neighbour joining method and default parameters. To map group-2b betacoronavirus sequence conservation onto the RBD structure, group-2b spike sequences were retrieved from GenBank and clustered using USEARCH[65] with a sequence identity threshold of 0.99, resulting in 39 clusters. For clusters of size >5, 5 spike sequences were randomly downsampled from each cluster. The resulting set of 73 sequences was aligned using MAFFT[66]. Conservation scores for each position in the multiple sequence alignment were calculated using the trident scoring method[67] and computed using the MstatX program (https://github.com/gcollet/MstatX). The conservation scores were then mapped to the RBD domain coordinates (PDB 7LD1) and images rendered with PyMol version 2.3.5.

Histopathology

Lung specimen from macaques were fixed in 10% neutral-buffered formalin, processed and blocked in paraffin for histology analyses. All tissues were sectioned at 5 µm and stained with haematoxylin and eosin to assess histopathology. Stained sections were evaluated by a board-certified veterinary pathologist in a blinded manner. Sections were examined under light microscopy using an Olympus BX51 microscope and photographs were taken using an Olympus DP73 camera.

Immunohistochemistry

Staining for SARS-CoV-2 nucleocapsid antigen was performed by the Bond RX automated system with the Polymer Define Detection System (Leica) following the manufacturer's protocol. Tissue sections were dewaxed with Bond Dewaxing Solution (Leica) at 72 °C for 30 min, then subsequently rehydrated with graded alcohol washes and 1× Immuno Wash (StatLab). Heat-induced epitope retrieval was performed using Epitope Retrieval Solution 1 (Leica) and by heating the tissue section to 100 °C for 20 min. A peroxide block (Leica) was applied for 5 min to quench endogenous peroxidase activity before applying the SARS-CoV-2 nucleocapsid antibody (1:2,000, GeneTex, GTX135357). Antibodies were diluted in Background Reducing Antibody Diluent (Agilent). The tissue was subsequently incubated with an anti-rabbit HRP polymer (Leica) and colorized with 3,3′-diaminobenzidine chromogen for 10 min. Slides were counterstained with haematoxylin.

Reagent authentication

Cell lines were received with a certificate of authentication certifying their identity. Cell identity was also confirmed by visualizing cell morphology and using flow cytometry to detect cell surface proteins. Cells were confirmed to be free of mycoplasma with monthly testing.

Statistics analysis

Data were plotted using Prism GraphPad 9.0. Wilcoxon rank-sum exact test was performed to compare differences between groups with P value <0.05, considered significant using SAS 9.4 (SAS Institute). No adjustments were made to the P values for multiple comparisons. The 50% and 80% inhibitory dilution (ID_{50} and ID_{80}, respectively) values were calculated using R statistical software (version 4.0.0). The R package 'nplr' was used to fit four-parameter logistic regression curves to the average values from duplicate experiments, and these fits were used to estimate the concentrations corresponding to 50% and 80% neutralization.

Reporting summary

Further information on research design is available in the Nature Research Reporting Summary linked to this paper.

Data availability

Data supporting the findings of this study are available within the Article and Supplementary Information. Any other relevant data are available from the corresponding authors upon reasonable request. Source data are provided with this paper.

51. Laczkó, D. et al. A single immunization with nucleoside-modified mRNA vaccines elicits strong cellular and humoral immune responses against SARS-CoV-2 in mice. *Immunity* **53**, 724–732.e7 (2020).
52. Pardi, N. et al. Zika virus protection by a single low-dose nucleoside-modified mRNA vaccination. *Nature* **543**, 248–251 (2017).
53. Wrapp, D. et al. Cryo-EM structure of the 2019-nCoV spike in the prefusion conformation. *Science* **367**, 1260–1263 (2020).
54. Hsieh, C.-L. et al. Structure-based design of prefusion-stabilized SARS-CoV-2 spikes. *Science* **369**, 1501–1505 (2020).
55. Zhou, T. et al. Structure-based design with tag-based purification and in-process biotinylation enable streamlined development of SARS-CoV-2 spike molecular probes. *Cell Rep.* **33**, 108322 (2020).
56. Berry, J. D. et al. Development and characterisation of neutralising monoclonal antibody to the SARS-coronavirus. *J. Virol. Methods* **120**, 87–96 (2004).
57. Coleman, C. M. & Frieman, M. B. Growth and quantification of MERS-CoV infection. *Curr. Protoc. Microbiol.* **37**, 15E.2.1–15.E.2.9 (2015).
58. Kint, J., Maier, H. J. & Jagt, E. Quantification of infectious bronchitis coronavirus by titration in vitro and in ovo. *Methods Mol. Biol.* **1282**, 89–98 (2015).
59. Naldini, L., Blömer, U., Gage, F. H., Trono, D. & Verma, I. M. Efficient transfer, integration, and sustained long-term expression of the transgene in adult rat brains injected with a lentiviral vector. *Proc. Natl Acad. Sci. USA* **93**, 11382–11388 (1996).
60. Yount, B. et al. Reverse genetics with a full-length infectious cDNA of severe acute respiratory syndrome coronavirus. *Proc. Natl Acad. Sci. USA* **100**, 12995–13000 (2003).
61. Scobey, T. et al. Reverse genetics with a full-length infectious cDNA of the Middle East respiratory syndrome coronavirus. *Proc. Natl Acad. Sci. USA* **110**, 16157–16162 (2013).
62. Hou, Y. J. et al. SARS-CoV-2 reverse genetics reveals a variable infection gradient in the respiratory tract. *Cell* **182**, 429–446.e14 (2020).
63. Wölfel, R. et al. Virological assessment of hospitalized patients with COVID-2019. *Nature* **581**, 465–469 (2020).
64. Yu, J. et al. DNA vaccine protection against SARS-CoV-2 in rhesus macaques. *Science* **369**, 806–811 (2020).
65. Edgar, R. C. Search and clustering orders of magnitude faster than BLAST. *Bioinformatics* **26**, 2460–2461 (2010).
66. Nakamura, T., Yamada, K. D., Tomii, K. & Katoh, K. Parallelization of MAFFT for large-scale multiple sequence alignments. *Bioinformatics* **34**, 2490–2492 (2018).
67. Valdar, W. S. Scoring residue conservation. *Proteins* **48**, 227–241 (2002).

Acknowledgements We thank V. Gee-Lai, M. Deyton, C. McDanal, B. Watts and K. Cronin for technical assistance; E. Donahue for program management and assistance with manuscript preparation; P. J. C. Lin and Y. K. Tam from Acuitas Therapeutics for providing lipid nanoparticles; J. Harrison, A. Granados, A. Goode, A. Cook, A. Dodson, K. Steingrebe, B. Bart, L. Pessaint, A. VanRy, D. Valentin, A. Strasbaugh and M. Cabus for assistance with macaque studies; and S. O'Connor and J. J. Baczenas at the Department of Pathology and Laboratory Medicine (University of Wisconsin-Madison) for sequencing support. The following reagent was deposited by the Centers for Disease Control and Prevention and obtained through BEI Resources, NIAID, NIH: SARS-CoV-2, isolate USA-WA1/2020, NR-52281. This work was supported by a grant from the State of North Carolina with funds from the federal CARES Act, by funds from NIH, NIAID, DAIDS grant AI142596 (B.F.H.), by support from the Ting Tsung & Wei Fong Chao Foundation (B.F.H.), by grant R01AI157155 (R.S.B.) and by grant U54 CA260543 (R.S.B.). This project was also supported by the North Carolina Policy Collaboratory at the University of North Carolina at Chapel Hill with funding from the North Carolina Coronavirus Relief Fund established and appropriated by the North Carolina General Assembly. This study was also supported by funding from an NIH F32 AI152296, a Burroughs Wellcome Fund Postdoctoral Enrichment Program Award, and was previously supported by an NIH NIAID T32

AI007151 (all three awarded to D.R.M.). COVID-19 sample processing was performed in the Duke Regional Biocontainment Laboratory, which received partial support for construction from the NIH/NIAD (UC6AI058607; G.D.S.) with support from a cooperative agreement with DOD/DARPA (HR0011-17-2-0069; G.D.S.).

Author contributions K.O.S. and B.F.H. designed and managed the study, reviewed all data and wrote and edited the manuscript; D.W. and N.P. designed and produced the mRNA-LNPs; E.L., A.M.S., F.C., H.C. and A.B.K. expressed proteins; S.K., J.T., H.G., E.L., R.P., M. Barr, T.H.O. III, D.R.M., D.C.M., L.V.T., T.D.S., G.D.S. and R.S.B. carried out binding, virus plaque and neutralization assays; R.S.B. and D.R.M. prepared recombinant live viruses encoding nLuc; D.L., C.T.D., T.N.D., M.G. and D.C.D. designed or performed sgRNA or genomic RNA assays; R.J.E., S.G., P.A., K. Mansouri, K. Manne, M.A., M. Berry and K.W. performed structural or sequence analysis; S.M.A. performed surface plasmon resonance; L.L.S., M.G.L., H.A. and R.S. and performed or evaluated macaque studies; K.W.B., M.M., B.M.N. and I.N.M. performed histology and immunochemistry; C.W.W., E.W.P. and G.D.S. collected and annotated COVID-19 samples; M.A.T. selected and provided adjuvant; C.B.F. formulated 3M052 in alum; R.W.R. and R.L.S. performed statistical analyses; all authors edited and approved the manuscript.

Competing interests B.F.H. and K.O.S. have filed US patents regarding the nanoparticle vaccine, M.A.T. and the 3M company have US patents filed on 3M052, and C.B.F. and IDRI have filed patents on the formulation of 3M052 and alum. The 3M company had no role in the execution of the study, data collection or data interpretation. D.W. is named on US patents that describe the use of nucleoside-modified mRNA as a platform to deliver therapeutic proteins. D.W. and N.P. are also named on a US patent describing the use of nucleoside-modified mRNA in lipid nanoparticles as a vaccine platform. All other authors declare no competing interests.

Additional information

Supplementary information The online version contains supplementary material available at https://doi.org/10.1038/s41586-021-03594-0.

Correspondence and requests for materials should be addressed to K.O.S. or B.F.H.

Peer review information *Nature* thanks Wolfgang Baumgärtner and the other, anonymous, reviewer(s) for their contribution to the peer review of this work. Peer reviewer reports are available.

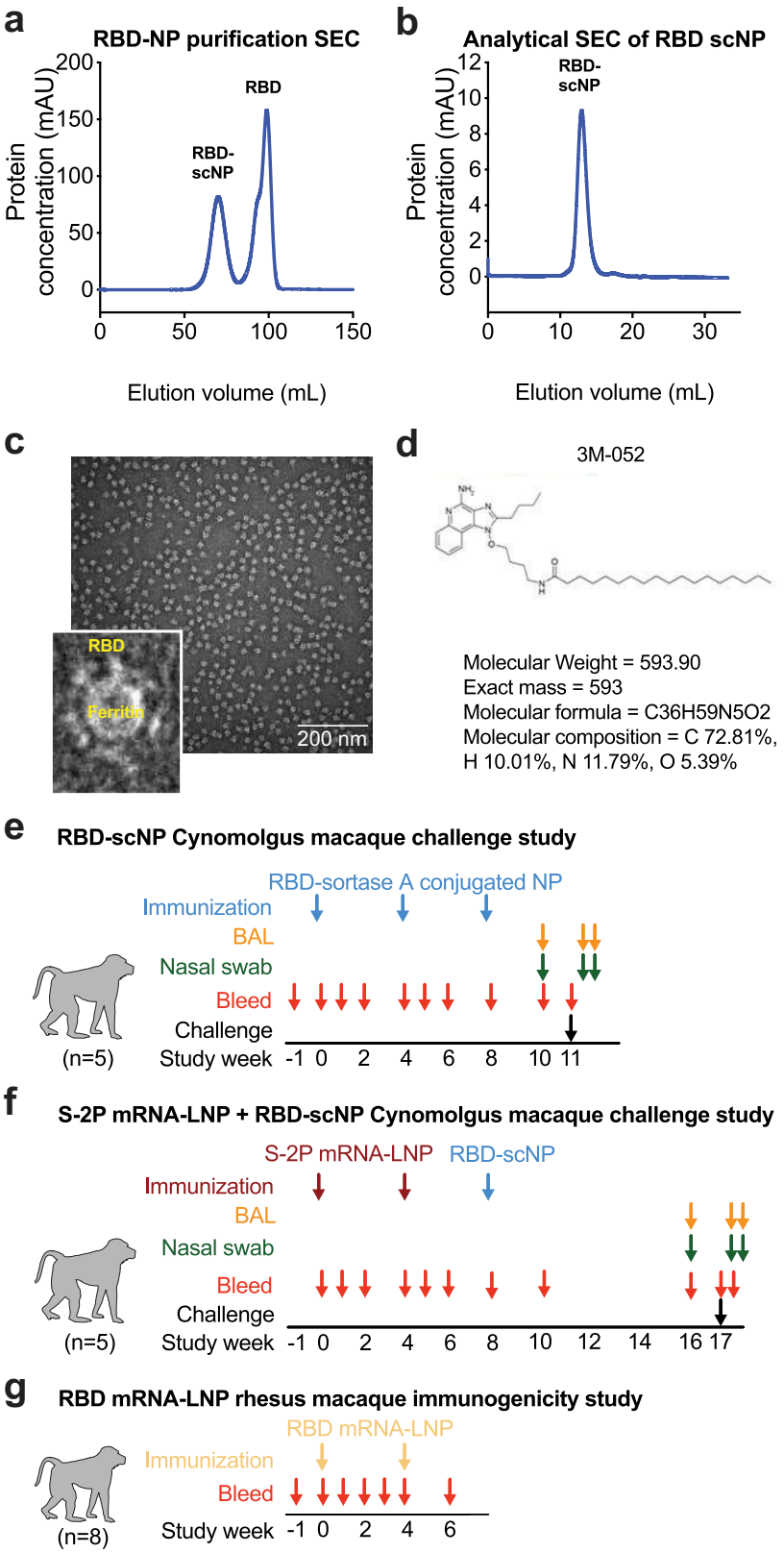

Extended Data Fig. 1 | See next page for caption.

Extended Data Fig. 1 | Molecular and structural characterization of the RBD–scNP. a, Size-exclusion chromatography of RBD and ferritin sortase conjugation. The first peak shows conjugated protein. The second peak contains unconjugated RBD. **b**, Analytical size-exclusion trace shows a homogenous nanoparticle preparation. **c**, Negative-stain electron microscopy image of RBD–scNP on a carbon grid. Inset shows a zoomed-in image of RBD–scNP. The zoomed image shows RBD molecules arrayed around the outside of the ferritin nanoparticle. A representative image from the 31 images taken of the micrograph to visualize 13,827 total particles is shown. **d**, Chemical structure of 3M-052. Alum formulation of 3M-052 was used to adjuvant RBD–scNP immunization. **e**, RBD–scNP immunization regimen used for vaccination of cynomolgus macaques ($n = 5$). Blue arrows indicate time points for intramuscular immunizations with RBD–scNP (100 μg) adjuvanted with 3M-052 (5 μg 3M-052 plus 500 μg alum). BAL (orange arrows) and nasal swab (green arrows) fluids were collected 7 days before, 2 days after and 4 days after intratracheal and intranasal SARS-CoV-2 challenge (black arrow). **f**, S-2P mRNA-LNP prime and RBD–scNP boost vaccination of cynomolgus macaques ($n = 5$). Burgundy arrows indicate time points for S-2P mRNA-LNP immunization (50 μg mRNA dose). Blue arrows are the same as in **a**. Macaques were challenged 9 weeks after RBD–scNP boost (week 17 of the study). BAL and nasal swab fluids were collected as in **a**. Macaques were challenged at week 17 (black arrow). **g**, RBD mRNA-LNP immunization of rhesus macaques ($n = 8$). Tan arrows indicate time points for RBD mRNA-LNP immunization (50 μg mRNA dose). Blood was collected throughout each study as shown by red arrows in all panels.

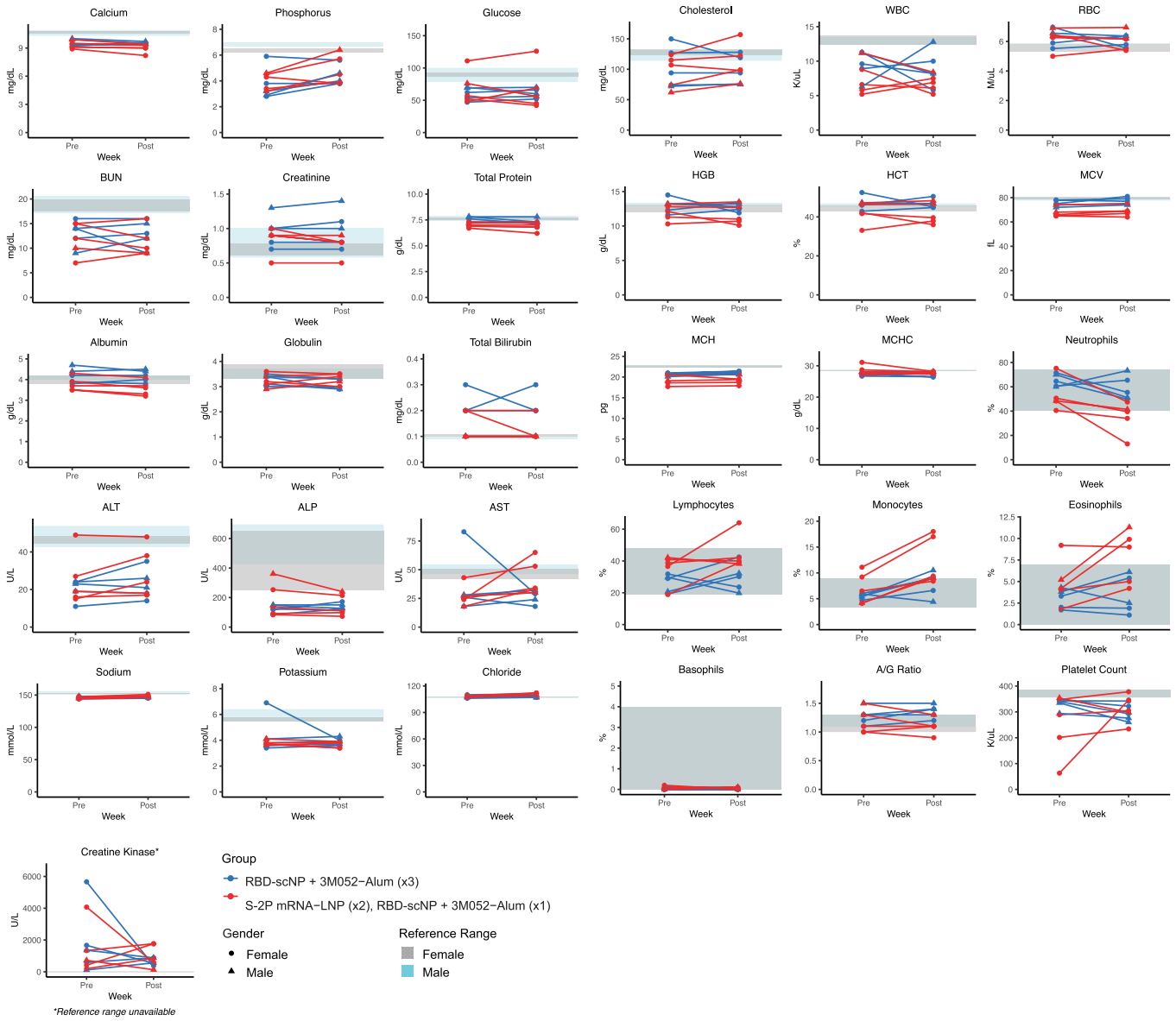

Extended Data Fig. 2 | Blood chemical analysis and blood cell counts in RBD−scNP- and S-2P mRNA-LNP-vaccinated macaques. Each graph shows values for individual macaques before vaccination and 4 weeks after the RBD−scNP (week 8) or 6 weeks after the second S-2P mRNA-LNP immunization (week 10). RBD−scNP-immunized macaques are shown as blue symbols, and S-2P mRNA-LNP-immunized macaques are shown as red symbols. The reference range for each value is shown as grey shaded area for female macaques and cyan shaded area for male macaques. Creatine kinase does not have a reference range indicated. Male macaques are shown as circles and female macaques are shown as triangles.

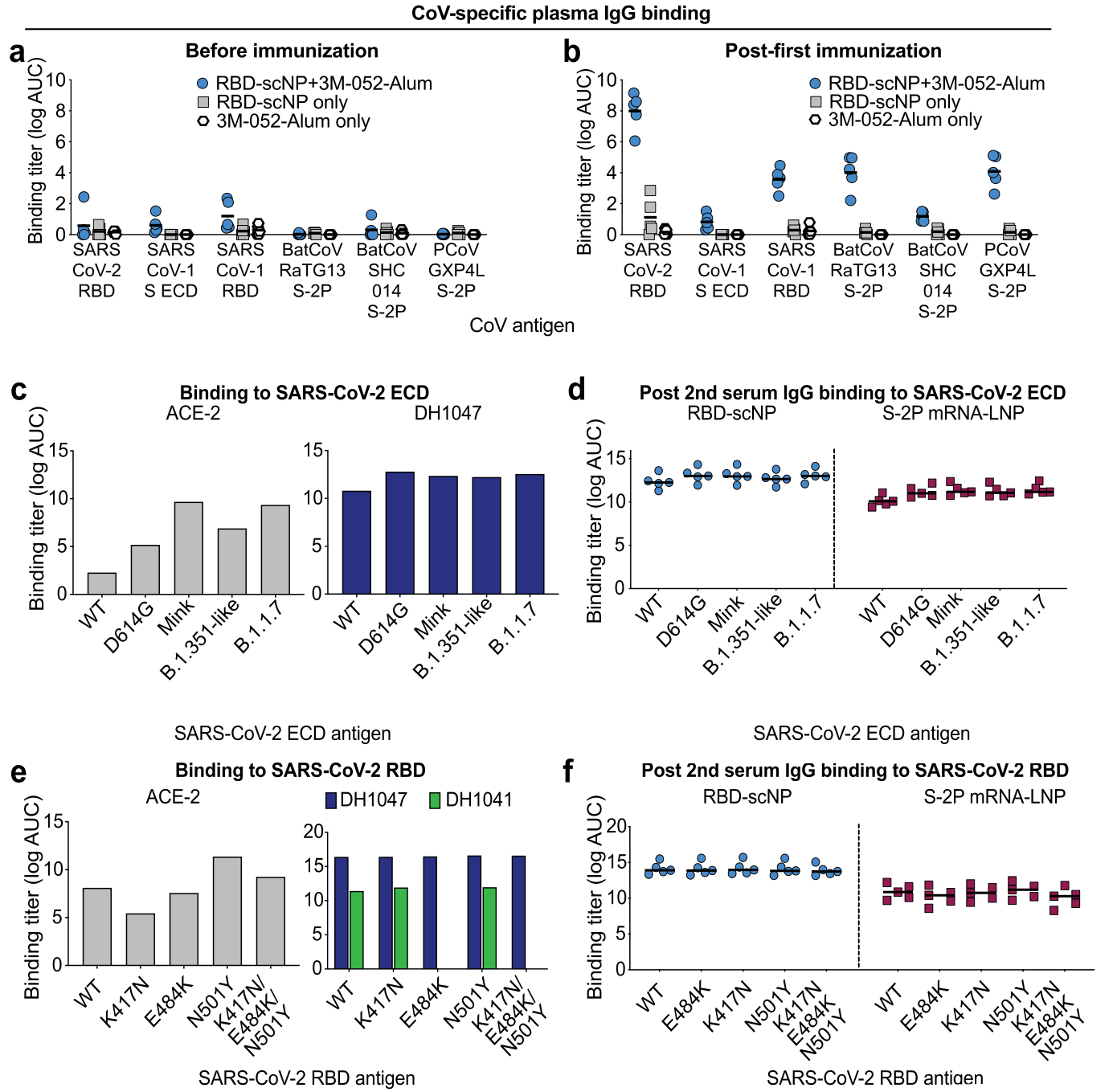

Extended Data Fig. 3 | ACE2, RBD neutralizing antibody and post-vaccination macaque plasma IgG binding to SARS-CoV-2 spike variants. a, **b**, Plasma IgG from macaques before immunization or after being immunized once with RBD–scNP adjuvanted with 3M-052 and alum (blue), RBD–scNP only (grey), or 3M-052 and alum only (white). Binding titres as log(AUC) were determined before (**a**) or two weeks after (**b**) a single immunization. Horizontal bars are the group mean. **c**, ACE2 receptor and cross-nAb DH1047 ELISA binding to SARS-CoV-2 spike ECD based on a Danish mink (H69/V70del/Y453F/D614G/I692V), B.1.351-like (K417N/E484K/N501Y/D614G) and B.1.1.7 (H69/V70del/Y144del/N501Y/A570D/D614G/P681H/T716I/S982A/D1118H) strains. Titres are shown as area under the log-transformed curve (log(AUC)). **d**, RBD–scNP- and S-2P mRNA-LNP-immunized macaque serum IgG ELISA binding to SARS-CoV-2 spike variants shown in **c**. Serum was tested after two immunizations. Horizontal bars are the group mean. **e**, ACE2 receptor (grey), cross-nAb DH1047 (navy) and ACE2-binding-site-targeting neutralizing antibody DH1041 (green) ELISA binding to SARS-CoV-2 spike RBD monomers. RBD variants contain a subset of mutations found in circulating B.1.351 and P.1 virus strains. Titres are shown as area under the log-transformed curve (log(AUC)). **f**, RBD–scNP- and S-2P mRNA-LNP-immunized macaque serum IgG ELISA binding to SARS-CoV-2 spike RBD variants shown in **e**. Serum was tested after two immunizations. Horizontal bars are the group mean.

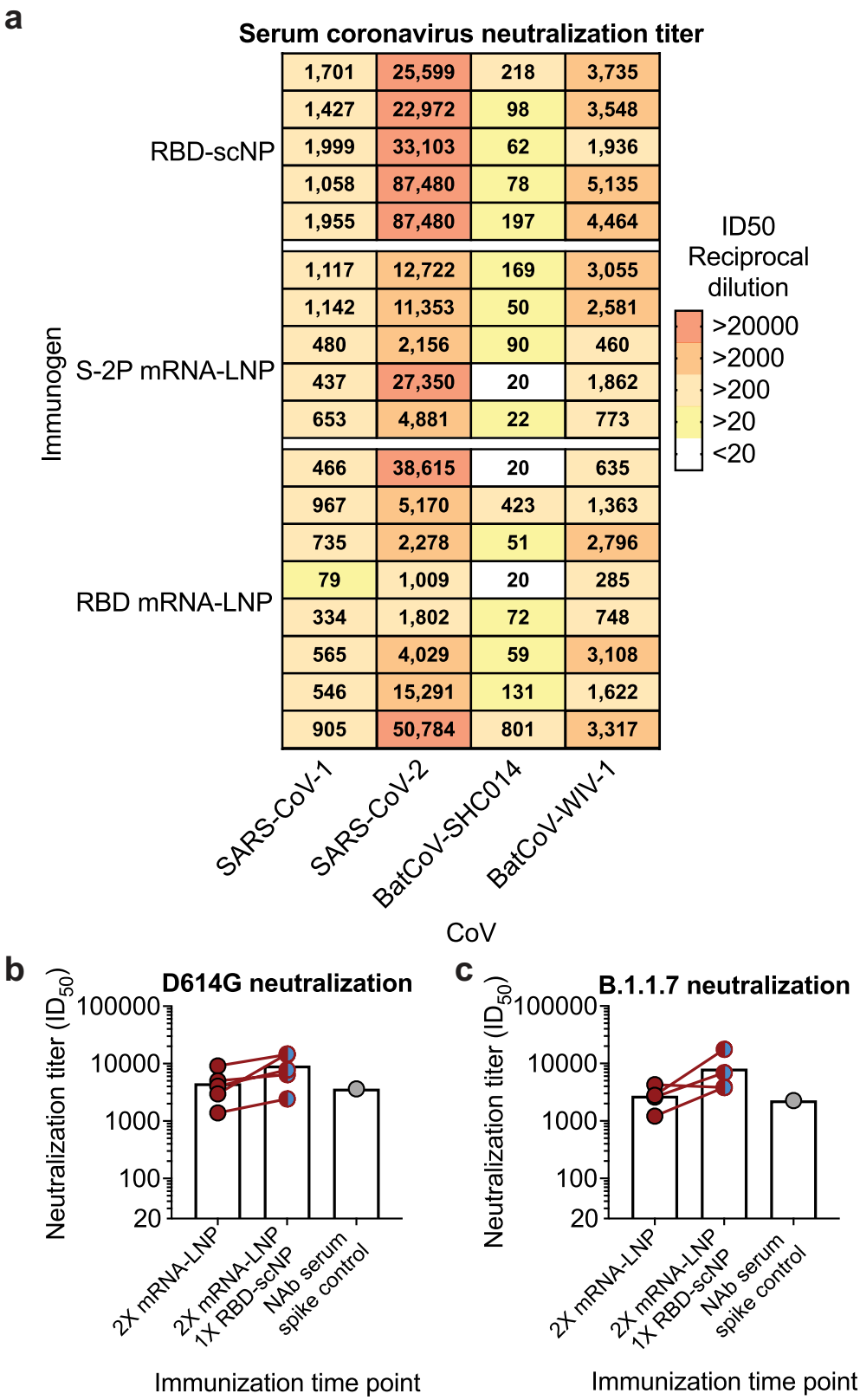

Extended Data Fig. 4 | Cross-nAbs are elicited by RBD–scNP and mRNA-LNP immunization. a, Each row shows neutralization titre for an individual macaque immunized with one of the three immunogens. A reciprocal serum dilution titre of 87,480 is the upper limit of detection and 20 is the lower limit of detection for this assay. Titres are derived from a nonlinear regression curve fit to the average of duplicate measurements. **b**, **c**, Serum neutralization titres elicited by two S-2P mRNA-LNP immunizations were boosted by a subsequent RBD–scNP immunization. Serum neutralization of SARS-CoV-2 D614G (**b**) and SARS-CoV-2 B.1.1.7 (**c**) pseudovirus infection of ACE2-expressing 293 cells. Neutralization titres are ID_{50} as reciprocal serum dilution for serum collected two weeks after the second (week 6) and third immunization (week 10). Each symbol connected by a line represents the titre for an individual macaque before and after RBD–scNP immunization. Normal human serum spiked with DH1043 was used as a positive control.

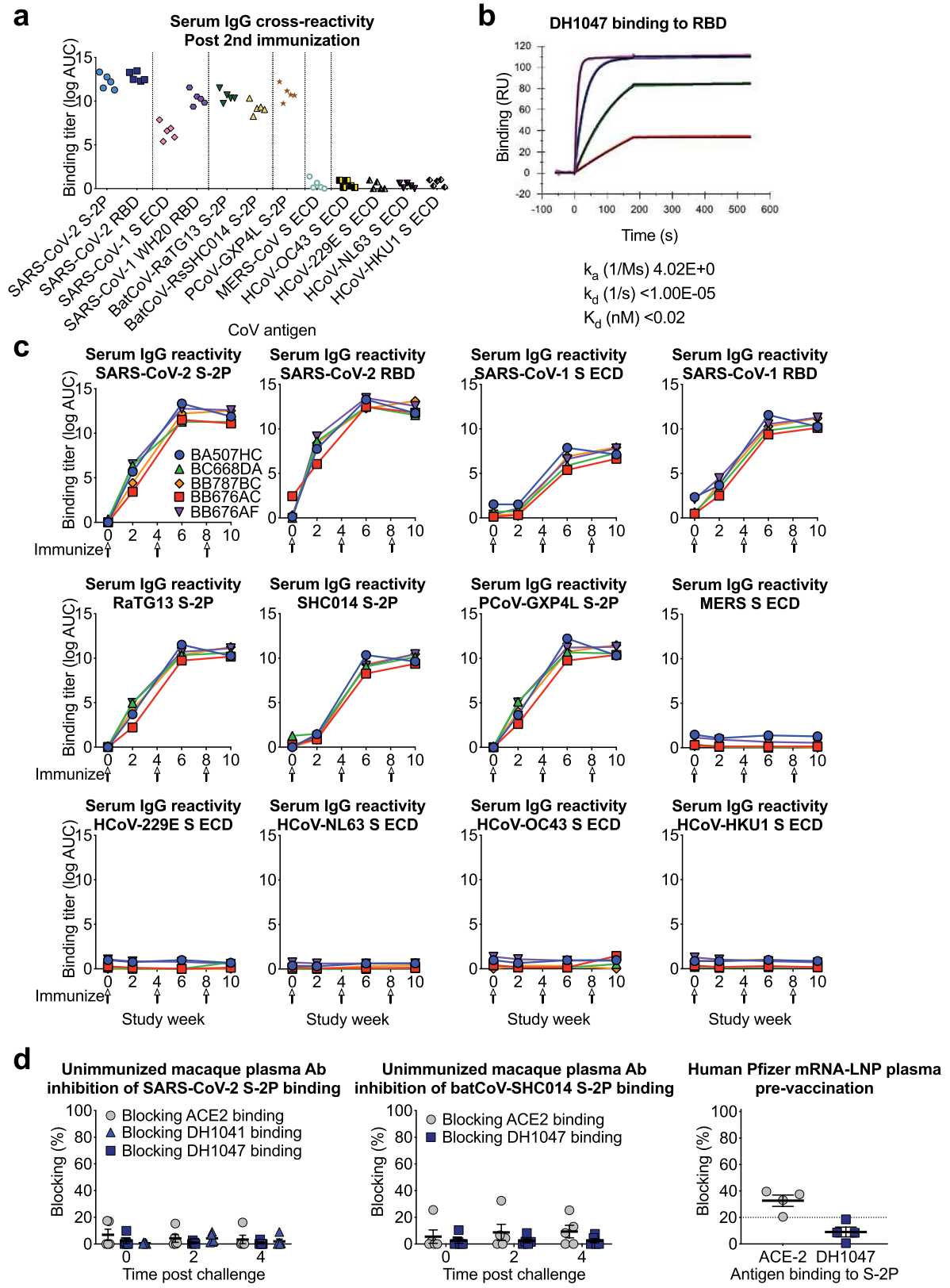

Extended Data Fig. 5 | Cross-reactive plasma antibody responses elicited by RBD–scNP immunization in macaques. a, Plasma IgG from macaques immunized twice with RBD–scNP binds to spike from human, bat and pangolin SARS-related coronavirus spike in ELISA, but not endemic human coronaviruses or MERS-CoV. **b**, Determination of DH1047 Fab binding kinetics to RBD monomer by surface plasmon resonance. Each curve shows a different concentration of DH1047 Fab. Binding kinetics are shown to the right from a 1:1 model fit. **c**, Time course of vaccinated macaque plasma IgG binding to human, bat and pangolin coronavirus spike protein by ELISA. Each curve indicates the binding titre for an individual macaque. Arrows indicate immunization time points. **d**, Unimmunized macaque plasma antibody blocking of SARS-CoV-2 S-2P (left) and SHC014 (middle) binding to ACE2, RBD neutralizing antibody DH1041 and RBD cross-nAb DH1047. Right, blocking activity in the serum of humans immunized with Pfizer BNT162b2 vaccine ($n = 4$). Each symbol represents an individual human or macaque. Bars indicate group mean ± s.e.m.

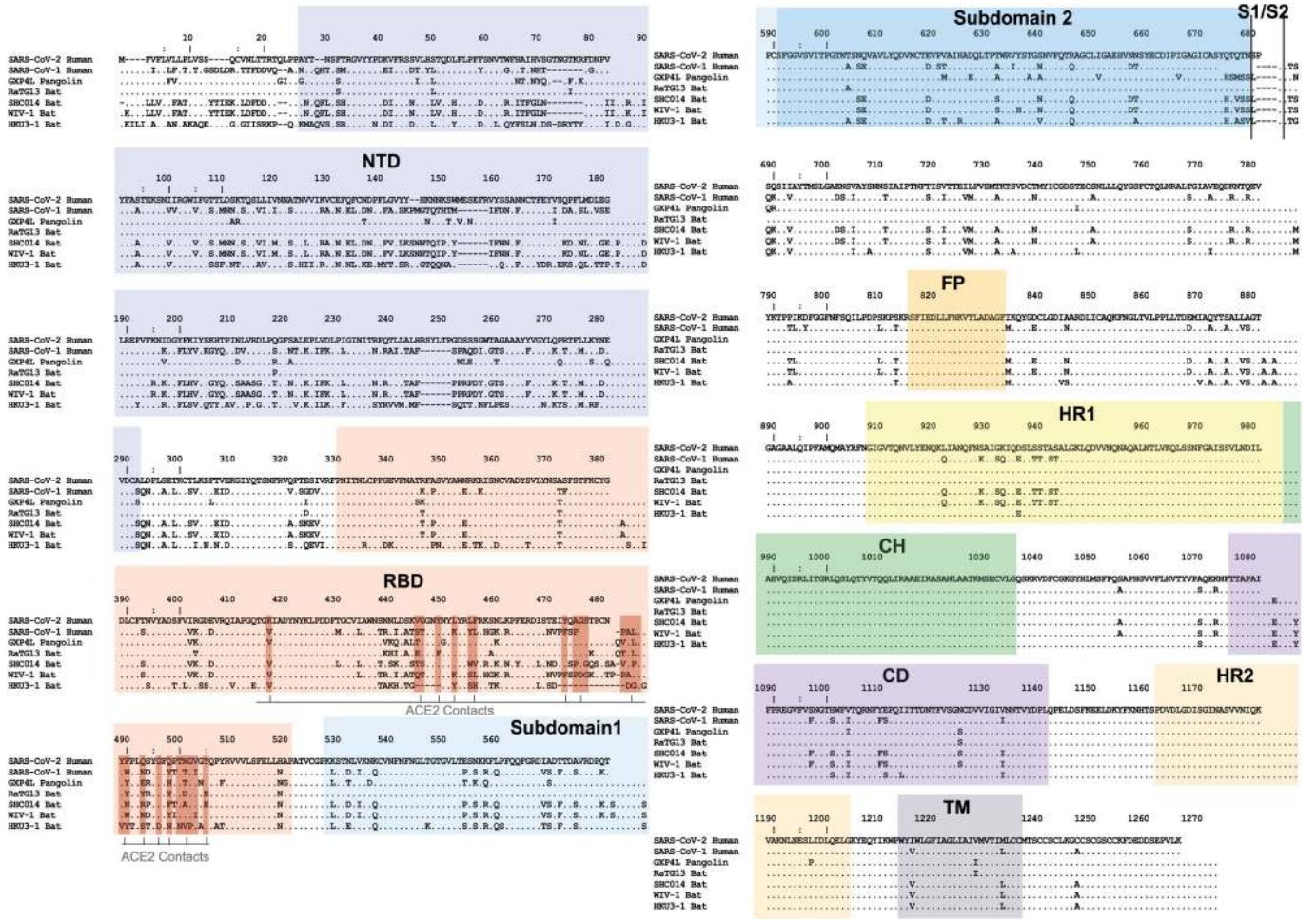

Extended Data Fig. 6 | Multiple sequence alignment of spike protein from a representative set of group 2b betacoronaviruses. SARS-CoV-2 Wuhan-1 spike protein numbering is shown. CD, connecting domain; CH, central helix; FP, fusion peptide; HR1, heptad repeat 1; HR2, heptad repeat 2; S1/S2, SARS-CoV-2 furin cleavage site; TM, transmembrane domain. ACE2 contact positions in SARS-CoV-2 (calculated from PDB coordinates 6MOJ and 6LZG) are highlighted in dark red.

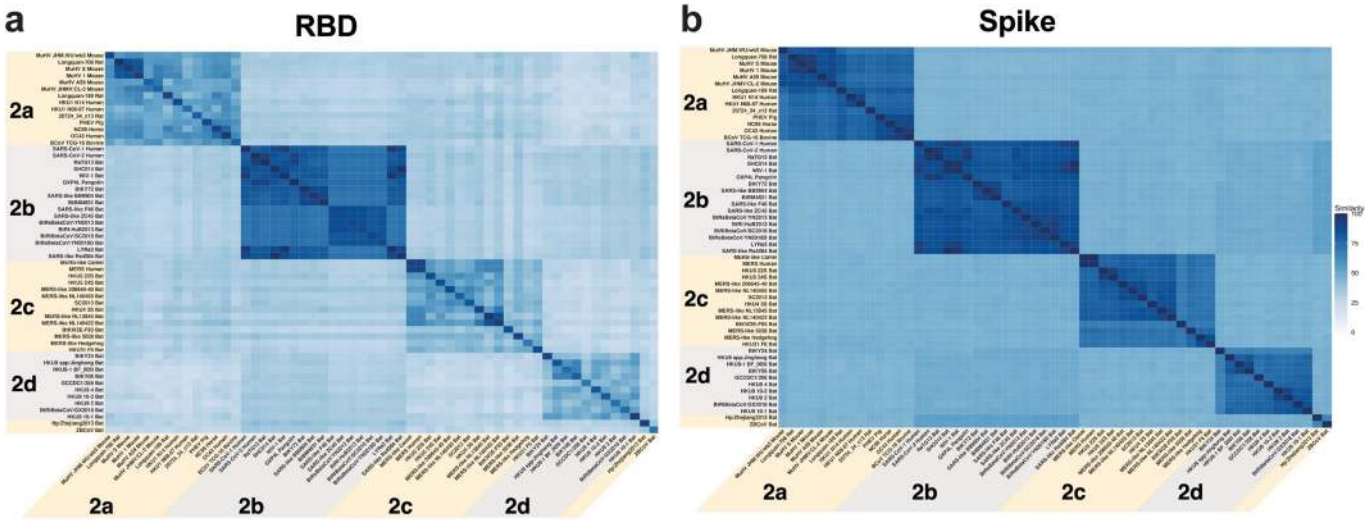

c

Group 2a
Longquan-708 Rat
MuHV S Mouse
MuHV 1 Mouse
MuHV A59 Mouse
MuHV JHMV/CL-2 Mouse
Longquan-189 Rat
HKU1 N14 Human
HKU1 N0S-87 Human
20724_34_C13 Rat
PHEV Pig
NC99 Horse
OC43 Human
BCoV TCG-16 Bovine

Group 2b
SARS-CoV-1 Human
SARS-CoV-2 Human
RaTG13 Bat
SHC014 Bat
WIV-1 Bat
GXP4L Pangolin
BtKY72 Bat
SARS-like BB9904 Bat
BtBM4831 Bat
SAAS-like F46 Bat
SAAS-like ZC45 Bat
BtRsBetaCoVIYN2013 Bat
BtRI-HuB2013 Bat
BtRIBetaCoV/SC2018 Bat
BtRsBetaCoV/YN2018D Bat
LVRa3 Bat
SARS-like As4084 Bat

Group 2c
MEAS-like Camel
MERS Human
HKU5 22S Bat
HKU5 24S Bat
MERS-like 206645-40 Bat
MEAS-like NL140455 Bat
SC2013 Bat
HKU4 3S Bat
MEAS-like NL13845 Bat
MEAS-like NL140422 Bat
BtKW2E-F93 Bat
MERS-like 5038 Bat
MEAS-like Hedgehog
HKU31 F6 Bat

Group 2d
BtKY24 Bat
HKU9 spp/Jinghong Bat
HKU9-1 BF_0051 Bat
BtKY06 Bat
GCCDC1I356 Bat
HKU9 4 Bat
HKU9 10-2 Bat
HKU9 2 Bat
BtRtBetaCoV/GX2018 Bat
HKU910-1 Bat

Ungrouped
Hp/ZheJlang2013 Bat
ZBCoV Bat

d

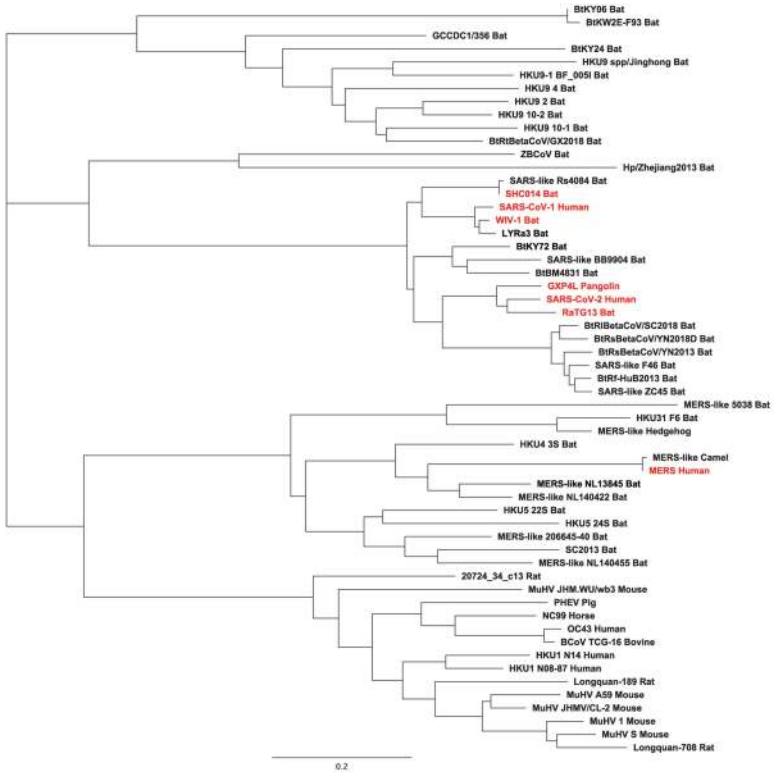

Extended Data Fig. 7 | Sequence conservation among SARS-related betacoronaviruses, MERS-CoV and endemic human coronaviruses. **a**, **b** Sequence similarity of RBD (**a**) and spike protein (**b**) for representative betacoronaviruses. Heat maps displaying pairwise amino acid sequence similarity for 57 representative betacoronaviruses. Dark blue shading indicates high sequence similarity. **c**, List of viruses used for alignments in **a**, **b** and Fig. 3f. **d**, Phylogenetic tree of representative betacoronavirus RBD sequences. Group 2b betacoronaviruses of interest are shown highlighted in red. Branch length units are substitutions per site.

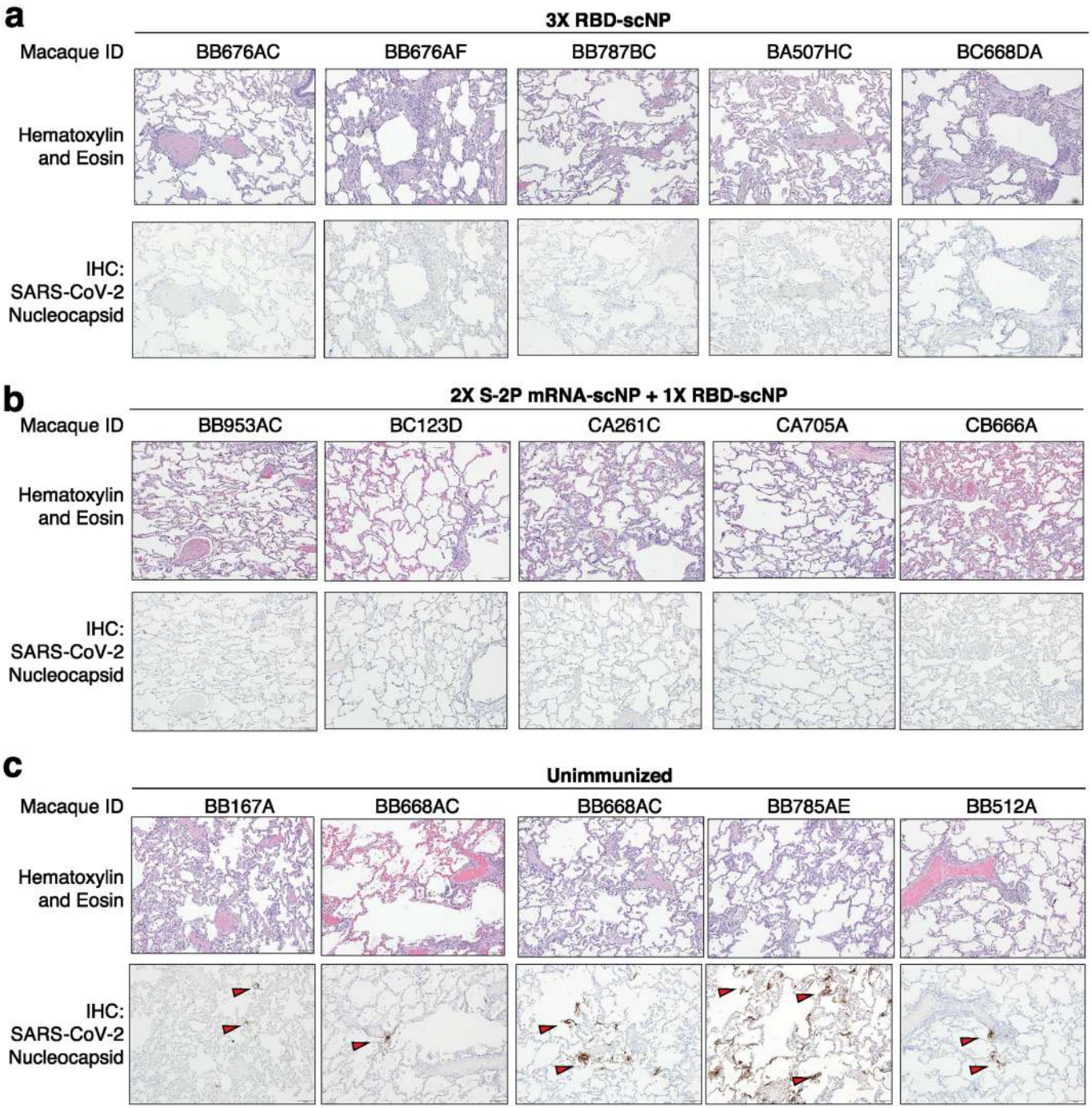

Extended Data Fig. 8 | Histology and immunohistochemistry of lung tissue collected seven days after SARS-CoV-2 WA-1 intratracheal and intranasal challenge. a–**c**, Macaques were immunized thrice with RBD–scNP (**a**), twice with S-2P mRNA-LNP and once with RBD–scNP (**b**) or not immunized (**c**). Each column shows results from an individual macaque. The macaque identification number is shown above each column. Haematoxylin and eosin stain of lung sections are shown on the top row, with nucleocapsid immunohistochemistry shown on the bottom row for each macaque. Red arrows indicate site of antigen positivity. All images are shown at 10× magnification. Scale bars, 100 µm.

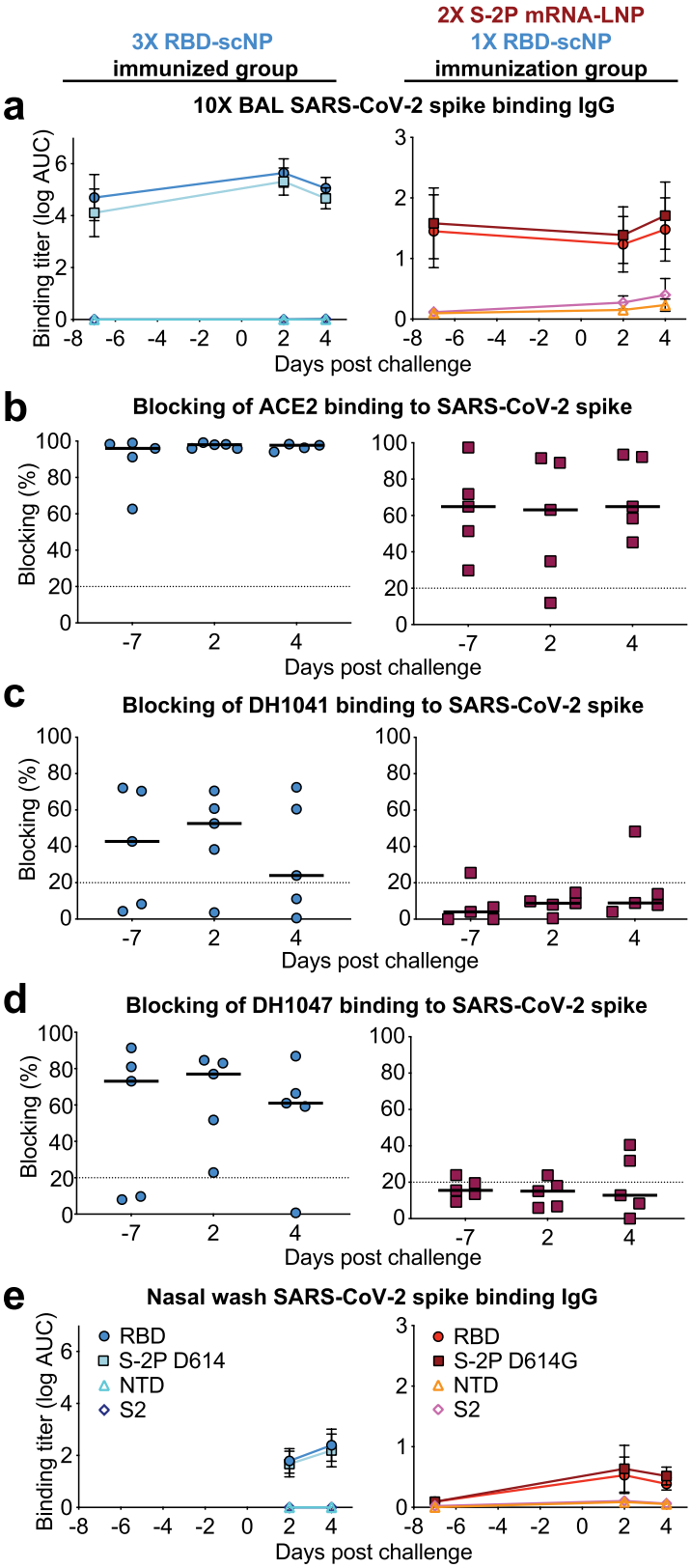

Extended Data Fig. 9 | See next page for caption.

Extended Data Fig. 9 | Mucosal SARS-CoV-2 IgG responses in BAL and nasal wash fluids before and after SARS-CoV-2 challenge. a, ELISA binding titres for SARS-CoV-2-specific IgG in 10× BAL fluid from macaques immunized with (blue symbols, left column) RBD–scNP three times or S-2P mRNA-LNP twice and RBD–scNP once (red symbols, left column). Day −7 BAL fluid was collected at week 10 or 16 for the RBD–scNP-alone group or the S-2P mRNA-LNP and RBD–scNP group, respectively. Group mean ± s.e.m. are shown ($n = 5$ macaques). **b**–**d**, The 10× BAL fluid blocking of ACE2, RBD neutralizing antibody DH1041 and cross-nAb DH1047 binding to SARS-CoV-2 D614G stabilized spike ectodomain. A black horizontal bar indicates the group mean blocking percentage. Blocking above 20% (above the dashed line) is considered positive. **e**, Neat nasal wash fluid from RBD–scNP-immunized or S-2P mRNA-LNP- and RBD–scNP-immunized macaques. Day −7 nasal wash fluid was collected at week 16 and 2 and 4 days after challenge for the S-2P mRNA-LNP and RBD–scNP group. Nasal wash fluid was unavailable for the RBD–scNP group before challenge, but was collected 2 and 4 days after the week-11 challenge. Group mean ± s.e.m. is shown ($n = 5$).

Extended Data Table 1 | Scoring of haematoxylin and eosin staining and immunohistochemistry of macaque lung tissue collected seven days after challenge

Group	Macaque ID	Tissue	H&E (Lc; Rm; Rc)	SARS-CoV-2 N IHC (Lc; Rm; Rc)
3X RBD-scNP	BB676AC	lung	+/-; +; +	-; -; -
	BB676AF	lung	++; ++; +	-; -; -
	BB787BC	lung	++; +; +	-; -; -
	BA507HC	lung	+; +; +/-	-; -; -
	BC668DA	lung	+/-; ++; ++	-; -; -
2X S-2P mRNA-LNP + 1X RBD-scNP	BB953AC	lung	+/-; +/-; +/-	-; -; -
	BC123D	lung	+/-; -; +/-	-; -; -
	CA261C	lung	+/-; +; +	-; -; -
	CA705A	lung	+/-; -; -	-; -; -
	CB666A	lung	+/-; +; +	-; -; -
Unimmunized	20201C	lung	+; +; +	+/-; -; -
	BB167A	lung	++; ++; ++	+/-; -; -
	BB668AC	lung	++; +; +	+/-; ++; ++
	BB785AE	lung	+/-; +++; +	-; ++; ++
	BB512A	lung	+; ++; ++	+; +/-; +

a, Haematoxylin and eosin (H&E) (inflammation). –, minimal to absent; +/–, minimal to mild; +, mild to moderate; ++, moderate to severe; +++, severe. **b**, Immunohistochemistry (IHC) (SARS-CoV-2 nucleocapsid antigen-positive foci). –, no SARS-CoV-2 antigen detected; +/–, rare or occasional; +, occasional or multiple; ++, multiple or numerous (and foci often larger); +++, numerous.

nature research

Corresponding author(s): Saunders, KO

Last updated by author(s): Feb 23, 2021

Reporting Summary

Nature Research wishes to improve the reproducibility of the work that we publish. This form provides structure for consistency and transparency in reporting. For further information on Nature Research policies, see Authors & Referees and the Editorial Policy Checklist.

Statistics

For all statistical analyses, confirm that the following items are present in the figure legend, table legend, main text, or Methods section.

n/a	Confirmed
☐	☒ The exact sample size (*n*) for each experimental group/condition, given as a discrete number and unit of measurement
☐	☒ A statement on whether measurements were taken from distinct samples or whether the same sample was measured repeatedly
☐	☒ The statistical test(s) used AND whether they are one- or two-sided *Only common tests should be described solely by name; describe more complex techniques in the Methods section.*
☒	☐ A description of all covariates tested
☐	☒ A description of any assumptions or corrections, such as tests of normality and adjustment for multiple comparisons
☐	☒ A full description of the statistical parameters including central tendency (e.g. means) or other basic estimates (e.g. regression coefficient) AND variation (e.g. standard deviation) or associated estimates of uncertainty (e.g. confidence intervals)
☐	☒ For null hypothesis testing, the test statistic (e.g. *F*, *t*, *r*) with confidence intervals, effect sizes, degrees of freedom and *P* value noted *Give P values as exact values whenever suitable.*
☒	☐ For Bayesian analysis, information on the choice of priors and Markov chain Monte Carlo settings
☒	☐ For hierarchical and complex designs, identification of the appropriate level for tests and full reporting of outcomes
☒	☐ Estimates of effect sizes (e.g. Cohen's *d*, Pearson's *r*), indicating how they were calculated

Our web collection on statistics for biologists contains articles on many of the points above.

Software and code

Policy information about availability of computer code

Data collection	No unique software was used for data collection.
Data analysis	Data were analyzed with commercially available and open-source programs as stated in the methods section. Descriptive statistics were calculated with Prism 8 and R program. Statistical tests were performed with SAS v9.4

For manuscripts utilizing custom algorithms or software that are central to the research but not yet described in published literature, software must be made available to editors/reviewers. We strongly encourage code deposition in a community repository (e.g. GitHub). See the Nature Research guidelines for submitting code & software for further information.

Data

Policy information about availability of data

All manuscripts must include a data availability statement. This statement should provide the following information, where applicable:

- Accession codes, unique identifiers, or web links for publicly available datasets
- A list of figures that have associated raw data
- A description of any restrictions on data availability

The authors declare that the data supporting the findings of this study are available within the main and supplemental figures. All data is available in the Source Data File.

Field-specific reporting

Please select the one below that is the best fit for your research. If you are not sure, read the appropriate sections before making your selection.

☒ Life sciences ☐ Behavioural & social sciences ☐ Ecological, evolutionary & environmental sciences

For a reference copy of the document with all sections, see nature.com/documents/nr-reporting-summary-flat.pdf

Life sciences study design

All studies must disclose on these points even when the disclosure is negative.

Sample size	We used groups of 5 or 8 macaques.
Data exclusions	No data were excluded.
Replication	Each binding study was repeated to confirm results. Within binding studies we tested multiple dilutions of antibodies to confirm the binding magnitude instead of relying on single data points. Neutralization assays have been validated to be reproducible and group geometric means are shown to identify the group trend.
Randomization	Macaques were distributed in groups to balance age, gender and weight whenever possible
Blinding	Neutralization, binding, and competition assays were performed by laboratories independent from the discovery laboratory. No other data was supplied until after the assay was complete. Statistics were not calculated until the study was complete, and were done so by statisticians independent from the discovery researchers.

Reporting for specific materials, systems and methods

We require information from authors about some types of materials, experimental systems and methods used in many studies. Here, indicate whether each material, system or method listed is relevant to your study. If you are not sure if a list item applies to your research, read the appropriate section before selecting a response.

Materials & experimental systems

n/a	Involved in the study
☒	☐ Antibodies
☐	☒ Eukaryotic cell lines
☒	☐ Palaeontology
☐	☒ Animals and other organisms
☒	☐ Human research participants
☒	☐ Clinical data

Methods

n/a	Involved in the study
☒	☐ ChIP-seq
☒	☐ Flow cytometry
☒	☐ MRI-based neuroimaging

Eukaryotic cell lines

Policy information about cell lines

Cell line source(s)	ThermoFisher and the Farzan Laboratory at Scripps
Authentication	Each cell line is provided with a certificate of analysis. Cell identity is verified by morphology or fluorescent markers expressed.
Mycoplasma contamination	All cell lines undergo mycoplasma testing every 60 days.
Commonly misidentified lines (See ICLAC register)	None to report.

Animals and other organisms

Policy information about studies involving animals; ARRIVE guidelines recommended for reporting animal research

Laboratory animals	Macca mulatta. Males and females were used in the studies. Macaques had various ages.
Wild animals	The study did not involve wild animals.
Field-collected samples	The study did not involve collection of samples from animals in the field.

Ethics oversight	The macaque studies were performed at Bioqual. Prior to study commencement, all procedures and materials to be used in the study were approved by the Bioqual IACUC. The Duke University Institutional Biosafety Committee approved protocols for research involving recombinant DNA.

Note that full information on the approval of the study protocol must also be provided in the manuscript.